

#### DEPARTMENT OF PHYSICS AND ASTRONOMY "A. RIGHI"

#### SECOND CYCLE DEGREE

#### **PHYSICS**

# Factorized Scattering Theories in 1+1Dimensions

Supervisor: Defended by:

Prof. Francesco Ravanini Ali Pazarci

#### Abstract

This thesis investigates whether S-matrices in 1+1 dimensional integrable quantum field theories remain valid at all energy scales or whether their thermodynamic behavior inevitably develops Hagedorn-like singularities that signal a scale where a breakdown of the S-matrix description occurs. We begin with a review of scattering theory and the role of integrability, emphasizing local conserved charges, factorizability, and the Yang-Baxter equation as central consistency conditions. Exact two-particle S-matrices are then constructed via the bootstrap program, providing the framework for analyzing both scattering amplitudes and thermodynamic behavior.

We paid close attention to the statistics of the particle spectrum in these integrable models, as the growth and distribution of states directly influence high-energy thermodynamics. Several examples are examined in detail. The examples include the sine-Gordon model as a standard example, the sausage model as a more intricate example, and higher-spin particle theories where a generalized S-matrix construction is developed through the quantum group symmetry algebra  $\mathcal{U}_q(\mathfrak{su}_2)$ . The spin 3/2 case is worked out explicitly. These examples allow for a systematic exploration of the validity of the S-matrix framework.

The analysis shows that while integrability permits exact control of scattering processes, the thermodynamic properties of certain models suggest potential limitations of the S-matrix description at extreme energies. These findings clarify the domain of validity of S-matrix theories and highlight the role of particle spectrum's statistics in determining whether such theories remain consistent or exhibit signs of Hagedorn-like behavior.

# Contents

	Abs	tract	3
1	Inti	roduction	7
2	S-N	Iatrices	15
	2.1	Review of The Scattering Theory	15
	2.2	S-matrices of integrable systems in 1+1 dimensions $\dots \dots$	17
		2.2.1 Local conserved charges and factorizability arguments	17
		2.2.2 The Yang-Baxter Equation	19
	2.3	Two-particle S-matrices	20
		2.3.1 The Bootstrap Equation	23
3	Examples of Factorized Scattering Theories in 1+1 Dimensions		27
	3.1	The Sine-Gordon Model	27
	3.2	The Sausage Model	31
	3.3	Exact Scattering Processes of The Higher-spin Particles	35
		3.3.1 The General S-matrix Construction	36
		3.3.2 The Spin $3/2$ Case	42
4	Cor	nclusion	51
Ribliography			60

Chapter 1

### Introduction

Scattering theory is a fundamental framework in physics that studies how particles or waves interact with a target, focusing on observable outcomes such as deflection angles, cross sections, and transition probabilities, and thereby connecting theory directly with experiment. In general scattering theory, many systems are too complex to solve exactly, so quantities like the S-matrix and phase shifts provide a practical way to predict outcomes and infer properties of interactions, as in Rutherford scattering or deep inelastic scattering, which revealed the nucleus and quark structure of protons. Integrable scattering theories in 1 + 1 dimensions, on the other hand, describe highly constrained systems with a large number of conserved quantities, where multi-particle scatterings factorize into sequences of two-particle scatterings without particle production or energy loss. This exact solvability allows physicists to compute precise S-matrices, correlation functions, and excitation spectra, particularly in 1+1 dimensional quantum systems and models. While general scattering theory provides the framework for understanding interactions and connecting with experiments across quantum mechanics, condensed matter, and particle physics, integrable scattering theories serve as exact examples that reveal the role of symmetry, conservation laws, and factorized dynamics, governing the scattering. Therefore, it offers deep insights into strongly interacting systems and guiding approximations in more complex non-integrable settings.

Integrable scattering theories are deeply connected to the mathematical structure of exactly solvable models through the Yang–Baxter equation and the bootstrap equations. Although the Yang-Baxter and bootstrap equations arise in different contexts, they embody the same fundamental principle, which is that self-consistency is crucial to determine the dynamics. The Yang–Baxter equation ensures the consistency of multi-particle scattering by guaranteeing that the order of sequential two-particle scatterings does not affect the final outcome, which is precisely why the factorization property holds in integrable systems. The bootstrap equations further constrain the theory by relating the bound states to the elementary particles, allowing one to compute their S-matrices consistently from the known two-particle scattering data. Together, these equations form the algebraic and analytic foundation of integrable models. They demonstrate that the solvability of such models is not a coincidence, but a reflection of deep structural constraints. We will contemplate three of such examples, which are the sine-Gordon model, the sausage model, and an example with higher-spin particles in this paper.

Firstly, the sine-Gordon model is an integrable quantum field theory in 1+1 dimensions, defined by the Lagrangian density

$$\mathcal{L}_{SG} = \frac{1}{2} (\partial \phi)^2 + \frac{m^2}{\beta^2} (\cos(\beta \phi) - 1) , \qquad (1.1)$$

where the coupling  $\beta$  controls the interaction strength. One should recall that we use the Minkowski flat metric, which has the minus sign convention for the time coordinate. Classically, it possesses a Lax pair and infinitely many conserved charges, and in the quantum theory, the integrability persists, which constitutes the scattering is purely elastic, no particle production occurs, and the multi-particle S-matrix factorizes into two-body processes. The spectrum consists of topological soliton and antisoliton excitations together with neutral bound states called breathers. Their corresponding breather masses are

$$M_k = 2M \sin \frac{\pi k}{h}$$
,  $k = 1, 2, \dots < \frac{8\pi}{\beta^2} - 1$  (1.2)

where  $h = \frac{16\pi}{\beta^2} \left(1 - \frac{\beta^2}{8\pi}\right)$  and M is the soliton mass. The exact two-particle S-matrix,

worked out by Zamolodchikov and Zamolodchikov in the late 1970s [7]. It depends only on the rapidity difference  $\theta = \theta_1 - \theta_2$  and satisfies unitarity, crossing symmetry, and the Yang-Baxter equation, while its pole structure encodes the bound-state spectrum. Explicit forms are given either as products of Gamma functions or as integral representations that make analytic properties transparent. Poles at

$$\theta = \left(1 - k\frac{2}{h}\right)\pi i, \quad k = 1, 2 \dots,$$

$$\theta = k\frac{2}{h}\pi i, \quad k = 1, 2 \dots,$$

$$(1.3)$$

$$\theta = k \frac{2}{h} \pi i, \quad k = 1, 2 \dots, \tag{1.4}$$

correspond to the breathers, with residues fixing their three-particle couplings [39]. The full multi-particle scattering is reconstructed from these two-body amplitudes by the bootstrap. This S-matrix underpins further exact constructions such as the form-factor program(see [32]) and the thermodynamic Bethe ansatz(see [25, 28, 35]). The former builds exact matrix elements of local operators and correlation functions, whereas the latter yields finite-temperature free energies and finite-volume spectra through nonlinear integral equations.

Secondly, in the sausage model, the target space is continuously deformed into an elongated, sausage-shaped surface by a single parameter, often written  $\nu$  or  $\lambda$ , instead of mapping the 2D spacetime into a perfectly round sphere. One crucial fact is that this deformation preserves the integrability, meaning the theory has infinitely many conserved quantities and highly constrained scattering [34]. In their 1993 work, Fateev, Onofri, and Zamolodchikov constructed two one-parameter families of such deformations (one family for the topological angle  $\theta = 0$  and the other for  $\theta = \pi$ ) and wrote down an exact, factorized S-matrix for the deformed theory that obeys unitarity, crossing symmetry, and the Yang-Baxter equation. These analytic scattering data allow one to compute physical quantities exactly in ways that are impossible for generic interacting field theories [34]. To check that the scattering description really corresponds to a deformed sigma model, they and subsequent authors used Bethe ansatz and thermodynamic Bethe ansatz (TBA) methods. These convert the S-matrix into equations for the finite-size energy levels and scaling func-

tions, showing that the sausage model indeed interpolates between known fixed points. It recovers the round O(3) model when the deformation parameter goes to zero and flows toward different behaviour in other limits. The geometric picture is tied to renormalization-group ideas where the sausage appears as an "ancient" solution of Ricci flow and is stable in two dimensions, where it flows back toward the round sphere, while analogous higher-dimensional sausages show instability [44]. On the quantum side, the integrable structure has been developed in several ways. Horváth and Takács used bootstrap-fusion techniques to relate the sausage model to sine-Gordon theory and constructed free-field representations and integral formulas for form-factors (the building blocks for correlation functions), which makes it possible to compute matrix elements of operators exactly [38]. More recently, researchers such as Bazhanov, Kotousov, and Lukyanov revisited the quantization using the ODE/IQFT (ordinary differential equation / integrable quantum field theory) correspondence and quantum inverse scattering ideas to obtain non-linear integral equations (NLIEs) for the model's quantum transfer matrices and vacuum eigenvalues, where they give a very precise handle on the spectrum and thermodynamics [47]. Altogether, the sausage model is valuable because it is a concrete, solvable example showing how nontrivial target space geometry and exact quantum solvability can coexist. It serves as a friendly toy model for methods like the Bethe ansatz, TBA, form-factor bootstrap, and ODE/IQFT. It has appeared repeatedly in connections to condensed matter spin chains, worldsheet sigma models in string theory, and mathematical studies of geometric flows [34, 38, 47].

Finally, an example with higher-spin particles is established in [54]. The authors construct the exact S-matrices for scattering theories where the asymptotic particles transform in higher-spin representations of the quantum group  $\mathcal{U}_q(\mathfrak{su}_2)$ . They begin with the ordinary  $\mathfrak{su}_2$  algebra, where particles carry spin s and corresponding magnetic quantum numbers  $m = -s, -s + 1, \ldots, s$ . The scattering of two such particles is encoded in a two-particle S-matrix that must satisfy three fundamental conditions, which are the Yang-Baxter equation, unitarity, and crossing

symmetry. To manage the structure, they decompose the two-particle Hilbert space into irreducible spin-J sectors by using projectors built from Clebsch–Gordan coefficients [36]. This decomposition allows them to parametrize the S-matrix as a sum of projectors weighted by scalar functions, where the latter are determined almost entirely by the Yang–Baxter equation, with only an overall scalar factor left undetermined. Then, they move from the rational case, where the underlying symmetry is the undeformed  $\mathfrak{su}_2$ , to the trigonometric case governed by the quantum group  $\mathcal{U}_q(\mathfrak{su}_2)$ . Here, the deformation parameter  $q=e^{2\pi i \gamma}$  is linked to the physical coupling constant. This generalization modifies both the representation theory and the structure of Clebsch–Gordan coefficients, which leads to q-deformed projectors and scalar functions. The authors of [26, 29] carefully derive the q-deformed Clebsch–Gordan coefficients, while in the [31], the subtleties that arise when q is a root of unity, where the expressions can diverge, are discussed. They show how to recover finite, consistent projectors in those cases using limiting procedures.

Once the structure of the S-matrix is established, unitarity and crossing symmetry are imposed to determine the overall scalar factor  $S_0(\theta)$ . As a result, formulas for this factor are written explicitly both when the spin s is an integer and when it is a half-integer. The integer spins are expressed in terms of products of hyperbolic functions, and in the more complicated half-integer case, they are expressed in terms of Gamma functions. Despite the apparent differences, both cases can be rewritten in a unified way through an integral representation, which highlights important physical properties. For instance, at the special value  $\gamma = 1/(2s)$ , the scalar factor reduces to -1, corresponding to a "free point" where the interactions vanish. In general, the resulting S-matrix is minimal, meaning that it does not contain CDD factors. In the range  $0 \le \gamma \le 1/(2s)$ , which corresponds to the repulsive regime, the theory does not have poles in the physical strip, meaning there are no bound states.

To illustrate this construction, we will work out in detail the author's examples and give the results for the case s = 3/2, which features four particle states labeled by the magnetic quantum numbers  $m = \pm 3/2, \pm 1/2$ . The nonvanishing S-matrix

elements are presented explicitly, and how they are built from the scalar prefactor and the q-deformed matrix part is shown. We verify that the full set respects the discrete symmetries of charge conjugation, parity, and time reversal. This example provides the first explicit S-matrix with nontrivial interactions for higher-spin particles beyond the well-known sine-Gordon (s = 1/2) and sausage (s = 1) models.

Then, we will see that their work establishes a family of exact, minimal S-matrices for arbitrary spin multiplets of  $\mathcal{U}_q(\mathfrak{su}_2)$ , in which all of them are consistent with the integrability requirements. These S-matrices serve as the starting point for the thermodynamic Bethe ansatz analysis, which is carried out in the same paper [54] by the authors, where they explore the thermodynamics and the emergence of Hagedorn-like singularities. In this thesis, we are investigating a question that arose from this observation.

In 1+1 dimensional integrable quantum field theories, the exact S-matrix encodes scattering data in a non-perturbative way, which is compatible with the bootstrap program, and enables one to derive thermodynamic quantities via the thermodynamic Bethe ansatz, even in the absence of a conventional Lagrangian. In many physical systems, such as the theory of hadrons and string theory, one still encounters a Hagedorn temperature, a threshold beyond which the canonical partition function diverges because the density of states grows exponentially [40].

Recent parallel advances in  $T\bar{T}$  deformations of integrable QFTs have shown that adding CDD factors to an S-matrix can induce a Hagedorn-like singularity in the finite-size energy E(R) obtained from the TBA. In these deformed theories, iterations of TBA equations break down below a critical scale  $R_*$ , and two branches of solutions merge in a square-root branch point, which is interpreted as a Hagedorn transition in the dual canonical interpretation [45, 46, 51].

These observations, together with the family of exact and minimal S-matrices in this thesis, motivate a deeper question. It is possible that the presence of a Hagedorn divergence is not merely an artifact of adding deformations or CDD factors, but is already hidden in the minimal exact S-matrix construction. If so, this would imply the existence of an intrinsic scale for the S-matrix description at high energies or temperatures. Therefore, one can ask [54]: do S-matrix theories remain valid at all energy scales, or do they intrinsically develop Hagedorn-like singularities in their thermodynamics that signal a breakdown of the S-matrix description? In this thesis, we will be investigating this question, as well as analyzing the consistency of these higher-spin S-matrices and the statistics of their particle spectrum.

 $_{ ext{Chapter}} 2$ 

## S-Matrices

#### 2.1 Review of The Scattering Theory

Let us consider an interacting theory, where we create initial and final states

$$|i\rangle, |f\rangle$$
 (2.1)

measured before and after the scattering. They are called asymptotic states if they are separated enough from the scattering point so that they behave like states in a free theory, usually referred as  $t \to \pm \infty$ . When we compute the transition probability of the initial state into the final state in the Heisenberg picture

$$\langle f | \hat{S} | i \rangle$$
, (2.2)

we make use of the operator  $\hat{S}$  called S-matrix. This picture with operator formalism is more convenient and widely used in quantum field theory (QFT) calculations. Due to the Heisenberg uncertainty principle, we will describe our states as wave packets distributed around some momentum  $p_i$ .

$$|\phi_i\rangle = \int \frac{d^3k}{(2\pi)^3} \frac{1}{\sqrt{2E_k}} \phi_i(\mathbf{k}) |\mathbf{k}\rangle,$$
 (2.3)

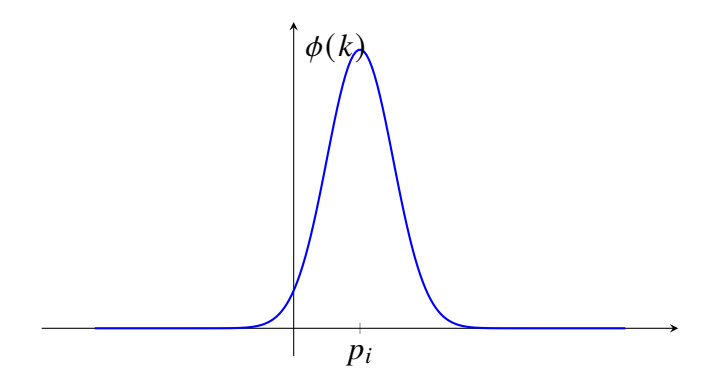


Figure 2.1: Distribution around  $p_i$ 

where  $\phi(\mathbf{k})$  is the Fourier transform of the wave function, and  $|\mathbf{k}\rangle$  is a one-particle state with momentum  $\mathbf{k}$ . We have the usual normalization conventions.

$$\langle \phi_i | \phi_i \rangle = \int \frac{d^3k}{(2\pi)^3} |\phi_i(\mathbf{k})|^2 = 1 \tag{2.4}$$

$$\langle \mathbf{k} | \mathbf{k'} \rangle = 2E_{\mathbf{k}} (2\pi)^{3} \delta(\mathbf{k} - \mathbf{k'})$$
 (2.5)

Let us now look at a  $2 \rightarrow n$  process.

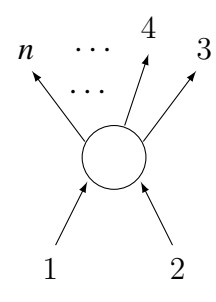


Figure 2.2: A  $2 \rightarrow n$  process represented diagrammatically

$$p_A + p_B \to p_1 + p_2 + \dots + p_n ,$$
 (2.6)

where we have the incoming states

$$|\phi_A \phi_B\rangle_{\rm in} = \int \frac{d^3 k_A}{(2\pi)^3} \frac{d^3 k_B}{(2\pi)^3} \frac{\phi_A(\mathbf{k}_A)\phi_B(\mathbf{k}_B)e^{-i\mathbf{b}\cdot\mathbf{k}_B}}{\sqrt{(2E_A)(2E_B)}} |\mathbf{k}_A \mathbf{k}_B\rangle_{\rm in} , \qquad (2.7)$$

where  $\boldsymbol{b} = \langle \phi_B | \boldsymbol{x}^{\perp} | \phi_B \rangle$  is the impact parameter, and the outgoing states

$$_{\text{out}}\langle \phi_1 \phi_2 \dots \phi_n | = \left( \prod_{i=1}^n \int \frac{d^3 p_i}{(2\pi)^3} \frac{\phi_i(\boldsymbol{p}_i)}{\sqrt{2E_i}} \right)_{\text{out}} \langle \boldsymbol{p}_1 \boldsymbol{p}_2 \dots \boldsymbol{p}_n | .$$
 (2.8)

Therefore, the mapping between the incoming and the possible outgoing states is given by

$$\langle \boldsymbol{p}_1 \boldsymbol{p}_2 \dots \boldsymbol{p}_n | \hat{S} | \boldsymbol{k}_A \boldsymbol{k}_B \rangle \tag{2.9}$$

If the particles were not interacting with each other,  $\hat{S}$  would simply be the identity operator. Since we are interested in the case where interactions are present, we can decompose the part where they play a role.

$$\hat{S} = \mathbb{I} + i\hat{T} \tag{2.10}$$

where  $\hat{T}$  is called the transfer matrix. This leads us to the definition of the invariant matrix element  $\mathcal{M}$  as follows.

$$\langle \boldsymbol{p}_1 \boldsymbol{p}_2 \dots \boldsymbol{p}_n | i \hat{T} | \boldsymbol{k}_A \boldsymbol{k}_B \rangle = (2\pi)^4 \delta^{(4)} \left( \boldsymbol{k}_A + \boldsymbol{k}_B - \sum_{i=1}^n \boldsymbol{p}_i \right) i \mathcal{M}$$
 (2.11)

We can find physical information in terms of these matrix elements, such as crosssections and decay rates, that are measured in a scattering experiment. Since we are focusing on the S-matrix part, we will not mention these applications here.

# 2.2 S-matrices of integrable systems in 1+1 dimensions

#### 2.2.1 Local conserved charges and factorizability arguments

Let us start by introducing some convenient definitions in 1+1 dimensional theories. The light-cone momentas, which satisfy the mass-shell condition  $p_a\bar{p}_a=m_a^2$ , are given by

$$p_a = p_a^0 + p_a^1 = m_a e^{\theta_a}$$
 ,  $\bar{p}_a = p_a^0 - p_a^1 = m_a e^{-\theta_a}$ , (2.12)

where  $(p_a^0, p_a^1) = (m_a \cosh \theta_a, m_a \sinh \theta_a)$  and  $\theta_a$  is the rapidity of the relevant particle. In this parametrization, the asymptotic state of n particles follows as

$$|A_{a_1}(\theta_1)A_{a_2}(\theta_2)\dots A_{a_n}(\theta_n)\rangle,$$
 (2.13)

where  $A_{a_n}(\theta_n)$  represents a particle of type  $a_n$  with the rapidity  $\theta_n$ .

The notion of being an asymptotic state and given collisions in 1 spatial dimension enables us to introduce a notation that indicates the ordering of the particles concerning their rapidities. We will benefit from this notation whenever we write the states out of the bra-ket notation like the following.

$$A_{a_1}(\theta_1)A_{a_2}(\theta_2)\dots A_{a_n}(\theta_n)$$
 , with  $\theta_1 > \theta_2 > \dots > \theta_n$  , (2.14)

$$A_{b_1}(\theta_1')A_{b_2}(\theta_2')\dots A_{b_n}(\theta_n')$$
 , with  $\theta_1' < \theta_2' < \dots < \theta_n'$  , (2.15)

for *in* and *out* states respectively. Here, we put the fastest particle on the left-hand side in the *in* states and on the right-hand side in the *out* states.

Factorizability of the S-matrices, together with no particle production and conservation of the initial and final momentas as a set, in an integrable theory is provided by the existence of infinitely many integrals of motion [9, 12] that are integrals of local densities and are in involution

$$Q_s = \int_{-\infty}^{\infty} \mathcal{T}_{s+1} dx \ . \tag{2.16}$$

Being in involution means the local conserved charges, as operators acting on the states,

$$Q_s |A_{a_1}(\theta_1) \dots A_{a_n}(\theta_n)\rangle = \sum_{i=1}^n \gamma_s^{a_i} e^{s\theta_i} |A_{a_1}(\theta_1) \dots A_{a_n}(\theta_n)\rangle$$
 (2.17)

are commuting.  $\gamma_s^{a_i}$  above are real numbers and satisfy  $\gamma_s^{a_i} = \gamma_{-s}^{a_i}$  due to parity invariance. s is called the Lorentz spin of  $Q_s$ .

Analyzing the action of such infinitely many  $Q_s$  on an  $n \to m$  amplitude

$$\gamma_s^{a_1} e^{s\theta_1} + \dots + \gamma_s^{a_n} e^{s\theta_n} = \gamma_s^{b_1} e^{s\theta_1'} + \dots + \gamma_s^{b_m} e^{s\theta_m'}, \qquad (2.18)$$

readily fixes  $n=m,\; \theta_i=\theta_i',\; {\rm and}\; \gamma_s^{a_i}=\gamma_s^{b_i} \; {\rm for}\; i=1\ldots n.$ 

Hence, our initial and final n-particle states in the notation of the equations (2.14) and (2.15) should be written as

$$A_{a_1}(\theta_1)A_{a_2}(\theta_2)\dots A_{a_n}(\theta_n) , \qquad (2.19)$$

$$A_{b_1}(\theta_n)A_{b_2}(\theta_{n-1})\dots A_{b_n}(\theta_1)$$
, (2.20)

respectively, where  $\theta_1 > \theta_2 > \cdots > \theta_n$  .

In particular, (Lorentz) spin |s| = 1 corresponds to conservation of the right and left lightcone momenta

$$\sum_{i=1}^{n} m_{a_i} e^{\theta_i} = \sum_{i=1}^{n} m_{b_i} e^{\theta_i} , \qquad (2.21)$$

$$\sum_{i=1}^{n} m_{a_i} e^{-\theta_i} = \sum_{i=1}^{n} m_{b_i} e^{-\theta_i} . {(2.22)}$$

Note that the coefficients are equal to the masses of the particles and the same for the values of  $s = \pm 1$ .

#### 2.2.2 The Yang-Baxter Equation

One can always utilize the commutative behavior of the  $Q_s$  and shift the initial and final configurations of the particles via a momentum-dependent phase factor without altering the scattering amplitude. This enables one to describe an n-particle scattering process as a chain of two-particle scattering processes, and the n-particle scattering amplitude as a product of n(n-1)/2 two-particle scattering amplitudes. We can also see that this factorization property says the order of the two-particle amplitudes doesn't affect the result, and therefore, gives an equivalence relation also known as the Yang-Baxter equation (YBE)

$$S_{ij}^{\beta\alpha}(\theta_{12})S_{\beta k}^{n\gamma}(\theta_{13})S_{\alpha\gamma}^{ml}(\theta_{23}) = S_{jk}^{\beta\gamma}(\theta_{23})S_{i\gamma}^{\alpha l}(\theta_{13})S_{\alpha\beta}^{nm}(\theta_{12}). \tag{2.23}$$

The Yang-Baxter equation is one of the most fundamental structures in the study of integrable models, with roots both in mathematical physics and pure mathematics. It was first introduced by C. N. Yang [3] in his study of one-dimensional many-body systems with factorized scattering, and independently by R. J. Baxter [4] in his solution of lattice models such as the eight-vertex model. Since its discovery, the YBE has become a cornerstone for integrability theory, quantum groups, and even knot theory [18, 22].

Mathematically, the YBE is an algebraic consistency condition for an operator R(u), called the R-matrix, which depends on a spectral parameter u. When acting

on a tensor product of three vector spaces  $V_1 \otimes V_2 \otimes V_3$ , the equation is usually written in the form

$$R_{12}(u-v)R_{13}(u-w)R_{23}(v-w) = R_{23}(v-w)R_{13}(u-w)R_{12}(u-v).$$

Here, the operator  $R_{ij}$  acts non-trivially on the *i*-th and *j*-th spaces while leaving the third space unchanged. The variables u, v, w represent spectral parameters that are often related to particle rapidities. This equation expresses the fact that two different sequences of pairwise interactions among three objects must lead to the same overall transformation.

Physically, the Yang–Baxter equation guarantees that in one-dimensional quantum systems, multiparticle scattering can always be factorized into successive two-body scattering processes. It asserts that no ambiguity arises from the order in which particles are made to interact, which is essential for integrability in 1+1 dimensional systems [11]. In the context of statistical mechanics, the YBE ensures that transfer matrices commute with one another for different values of the spectral parameter, a property that enables exact solutions of lattice models such as the six-vertex and eight-vertex models [15].

The influence of the YBE extends far beyond statistical mechanics and scattering theory. In mathematics, it plays a central role in the theory of quantum groups developed by Drinfeld [18] and Jimbo [22], providing the algebraic backbone for their definition. In topology, the R-matrix solutions of the YBE lead to braid group representations, linking integrable systems to knot invariants like the Jones polynomial [19]. One can conclude that the YBE serves as a unifying bridge across physics and mathematics, embodying the principle that consistency of interactions at a local level dictates the solvability of the global system.

#### 2.3 Two-particle S-matrices

Since we have deduced that the knowledge of n-particle scattering processes can be constructed from two-particle scattering processes in integrable theories, studying

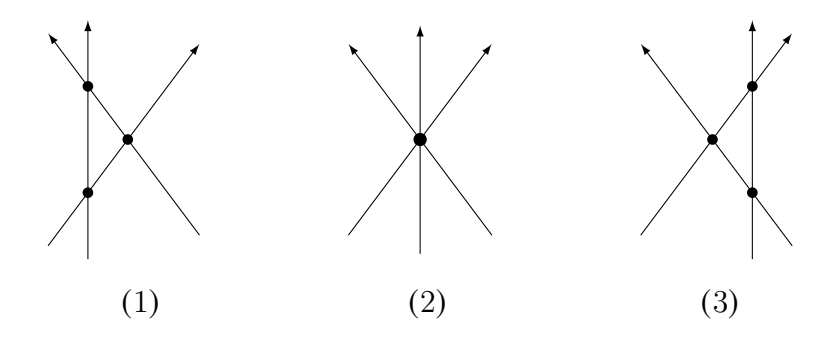


Figure 2.3: A  $3 \rightarrow 3$  process at tree level, equality between (1) and (3) constitutes the Yang-Baxter equation (2.23).

their two-particle scattering matrix became the main objective of the story.

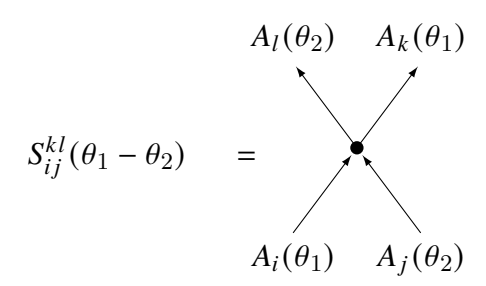


Figure 2.4: The two-particle S-matrix

Keeping our notation in the previous section in mind, the two-particle scattering matrix can be written as

$$A_{a_i}(\theta_1)A_{a_j}(\theta_2) = S_{ij}^{kl}(\theta_{12})A_{a_l}(\theta_2)A_{a_k}(\theta_1) , \qquad (2.24)$$

where  $\theta_1 > \theta_2$  and  $\theta_{12} = \theta_1 - \theta_2$ .

We can start determining the matrix elements in (2.24) by requiring the process to satisfy the discrete symmetries C, P, and T as physical theories usually do.

- $\bullet$  Charge conjugation:  $S^{kl}_{ij}(\theta) = S^{\bar{k}\bar{l}}_{\bar{i}\bar{j}}(\theta)$
- $\bullet$  Parity inversion:  $S_{ij}^{kl}(\theta) = S_{ji}^{lk}(\theta)$
- $\bullet$  Time reversal:  $S_{ij}^{kl}(\theta) = S_{lk}^{ji}(\theta)$

Furthermore, We can deduce important constraints on the S-matrix as well as information about its functional form from its analytical continuation. The continuation is usually carried out in Mandelstam variables

$$s = (p_1 + p_2)^2$$
,  $t = (p_1 - p_3)^2$ ,  $u = (p_1 - p_4)^2$ , (2.25)

where  $s+t+u=\sum_{i=1}^4 m_i^2$  and  $p_i=(p_i^{(0)},p_i^{(1)})=(E_i,p_i^{(1)})$ . Equivalently, we can write them in terms of rapidity  $\theta$  by recalling our parametrization (2.12) as the following.

$$s = m_1^2 + m_2^2 + 2m_1 m_2 \cosh \theta_{12}$$
 (2.26)

$$t = m_1^2 + m_3^2 - 2m_1 m_3 \cosh \theta_{13} \tag{2.27}$$

$$u = m_1^2 + m_4^2 - 2m_1 m_4 \cosh \theta_{14}$$
 (2.28)

We have only one linearly independent variable among them. The variable s is chosen conveniently in most of the literature as we will do. In this particular case, we can set  $p_3 = p_2$  and  $p_4 = p_1$  such that  $t = (p_1 - p_2)^2 = 2m_1^2 + 2m_2^2 - s$  and u = 0.

The physical values of s, corresponding real rapidity difference  $\theta_{12}$ , are given by  $s \ge (m_1 + m_2)^2$ , and defined as  $s^+ = s + i0$  on the s-plane. Analytical continuation results in two branch cuts on the branch points  $s = (m_1 + m_2)^2$  and  $s = (m_1 - m_2)^2$  as  $s \ge (m_1 + m_2)^2$  and  $s \le (m_1 - m_2)^2$ . It can be seen that it is a single-valued meromorphic function and is real analytic, which means  $S_{ij}^{kl}(s^*) = \left[S_{ij}^{kl}(s)\right]^*$ . The sheet that contains the physical values is called the physical sheet.

Additionally, we are going to consider two important assumptions for a physical theory, namely, the unitarity and crossing symmetry. After we determine their form in s-plane, we will express them in  $\theta$  parametrization to make them simpler and more useful for the context. Unitarity tells us

$$S_{ij}^{kl}(s^{+}) \left[ S_{kl}^{nm}(s^{+}) \right]^{*} = S_{ij}^{kl}(s^{+}) S_{kl}^{nm}(s^{-}) = \delta_{i}^{n} \delta_{j}^{m}, \qquad (2.29)$$

where  $s^- = s - i0$ . In particular, if we take the discrete symmetries into consideration, we arrive at

$$S_{ij}^{kl}(s^+)S_{ij}^{kl}(s^-) = 1. (2.30)$$

Next, the crossing symmetry states the equality of the amplitudes on the crossed channel t. For the physical values, we have

$$S_{ij}^{kl}(s^{+}) = S_{i\bar{l}}^{k\bar{l}}(t^{+}) = S_{i\bar{l}}^{k\bar{l}}(2m_{1}^{2} + 2m_{2}^{2} - s^{+}), \qquad (2.31)$$

where  $t^+ = t|_{s=s^+}$  are the physical values on the crossed channel. As we promised, it is now time to switch back to  $\theta$  parametrization via equation (2.26).

$$\theta_{12} = \cosh^{-1}\left(\frac{s - m_1^2 - m_2^2}{2m_1 m_2}\right) \tag{2.32}$$

$$= \log \left[ \frac{1}{2m_1m_2} \left( s - m_1^2 - m_2^2 + \sqrt{(s - (m_1 + m_2)^2)(s - (m_1 - m_2)^2)} \right) \right]$$
(2.33)

This transforms the physical sheet into the so-called physical strip  $0 \le \text{Im}(\theta_{12}) \le \pi$  on the  $\theta$ -plane Fig.(2.5). After looking at the  $\theta$ -plane, it can be realized that  $S(\theta)$  is

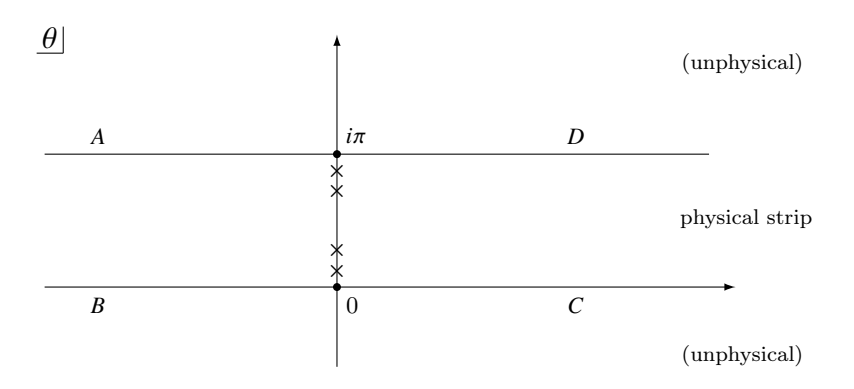


Figure 2.5: The  $\theta$  plane

real for the  $\theta$  values on the imaginary axis. As a result of what we have done so far, the constraints on the S-matrix we found by the analytical continuation in terms of the Mandelstam variables lead to the following constraints in terms of rapidity.

- $\bullet$  Unitarity:  $S_{ij}^{nm}(\theta)S_{nm}^{kl}(-\theta)=\delta_i^k\delta_j^l$

Here, our goal is to construct the two-particle S-matrix of our theory to solve all the n-particle scattering amplitudes. These constraints will guide us through the determination of such an S-matrix since they impose strong conditions on it.

#### 2.3.1 The Bootstrap Equation

The bootstrap equation has a powerful physical significance. It guarantees that once a small set of fundamental scattering amplitudes is known, the amplitudes involving bound states follow automatically. This means that the full particle spectrum of a model can be generated iteratively from a small starting point, provided the bootstrap principle holds. it restricts the possible S-matrices so severely that in many cases the exact scattering theory can be determined completely [11, 42].

In two-dimensional integrable quantum field theory, scattering processes are highly constrained because of factorization. The bootstrap equation typically comes into play when bound states appear in the spectrum. Therefore, one should be aware that this S-matrix has to be the exact S-matrix, which contains all the physical particles (not the virtual particles) in the theory's particle spectrum. To do so, one should study the pole structure of the S-matrix in hand and introduce the new particles as bound states on the poles on the physical strip. The position of each pole simply tells us the rapidity difference (and therefore the fusing angle, see below) where the new particle will be formed.

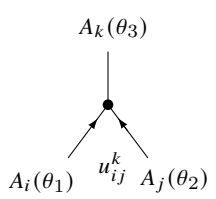


Figure 2.6: The particles of type i and j fuses into a stationary bound state of type k at  $\theta = iu_{ij}^k$ 

In order to make the S-matrix complete, we need to find the scattering amplitudes of this new particle. To do so, we can utilize the following bootstrap equation for diagonal S-matrices since they are required to be diagonal after we indicate all the non-zero higher spin conserved charges.

$$S_{lk}(\theta) = S_{li}(\theta - i\bar{u}_{ki}^{j})S_{lj}(\theta + i\bar{u}_{jk}^{i}) , \qquad (2.34)$$

where l is a particle scattering with  $\bar{k}$  formed by the fusing of i and j with the fusing angles  $\bar{u}_{ij}^k = \pi - u_{ij}^k$  and  $u_{ij}^k$ , determined by the kinematics of the bound-state formation, where  $\theta_{ij} = iu_{ij}^k$ . The equation asserts that the amplitude for the

bound state scattering is exactly equivalent to the product of the amplitudes of its constituents, with appropriately shifted rapidities.

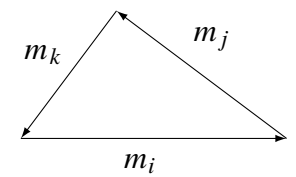


Figure 2.7: The mass triangle

The mass of the particle k follows from

$$s = m_k^2 = m_i^2 + m_j^2 + 2m_i m_j \cos u_{ij}^k , \qquad (2.35)$$

which already looks similar to the cosine theorem, but differs by a minus sign in the last term.

As a result, it has a geometric interpretation of fusing angles as outer angles of the so-called mass triangle Fig.(2.7) and gives

$$u_{ij}^k + u_{ik}^i + u_{ki}^j = 2\pi . (2.36)$$

Moreover, we can extend the equation (2.17) for the complex rapidities and consider the action of  $Q_s$  on a fusing process to generalize (2.35) further, which is called the generalized mass triangle Fig.(2.8).

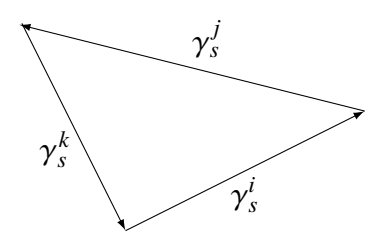


Figure 2.8: The generalized mass triangle

$$\gamma_s^k = \gamma_s^i e^{is\bar{u}_{ki}^j} + \gamma_s^j e^{-is\bar{u}_{kj}^i} , \qquad (2.37)$$

where we picked  $\theta_1 = \bar{u}_{ki}^j$  and  $\theta_2 = -\bar{u}_{kj}^i$ . They give a condition on the numbers representing the action of  $Q_s$  without specifying a local density. The equations (2.37) are known as the conserved charge bootstrap equations.

The bootstrap equation (2.34) arises from a different but equally powerful consistency principle like YBE (2.23). Its origins lie in the bootstrap program of the 1960s, which proposed that strongly interacting particles should be viewed as composites of one another with no fundamental constituents [2]. This bootstrap philosophy survived and remains central in the study of integrable quantum field theories, particularly in two dimensions. It has far-reaching implications in both physics and mathematics. In integrable quantum field theories such as the sine-Gordon model and affine Toda field theories, it is the essential tool for determining the full spectrum of bound states and their scattering properties [17, 30]. In more modern developments, the bootstrap philosophy has been generalized beyond two dimensions to the so-called conformal bootstrap and numerical bootstrap, where self-consistency conditions on correlation functions replace those on scattering amplitudes. These approaches have yielded highly non-trivial results in the study of conformal field theories, critical phenomena, and strongly coupled quantum systems [41, 49].

Chapter 3

# Examples of Factorized Scattering

## Theories in 1+1 Dimensions

#### 3.1 The Sine-Gordon Model

The sine-Gordon model is a nonlinear field theory that has roots reaching back to the 19th century. Its general description is given by the following equation.

$$\frac{\partial^2 \phi}{\partial t^2} - \frac{\partial^2 \phi}{\partial x^2} + \sin \phi = 0 \tag{3.1}$$

This was first studied in a purely mathematical context in the 1860s by Ferdinand Minding, and later Albert Bäcklund and Luther Pockels in connection with problems in differential geometry. In particular, it described the Gaussian curvature of surfaces of constant negative curvature. This geometric interpretation was eventually rediscovered in the 20th century.

It gained prominence in the 1960s and 1970s as part of a broader interest in nonlinear wave equations and solitons [5, 16, 20, 21]. This interest was catalyzed by advances in computational methods and the inverse scattering transform (IST)[14], developed in the context of the Korteweg-de Vries (KdV) equation.

In 1971, G. L. Lamb, M. Ablowitz, D. Kaup, and others showed that the sine-Gordon equation is integrable, meaning it admits an infinite number of conserved

quantities and exact soliton solutions. This sparked a flurry of research on integrable models and their rich mathematical structures. It appears as one of the 1+1-dimensional scalar field theories, although often as a toy model, to study non-perturbative phenomena like topological solitons and kinks. The sine-Gordon equation in soliton theory supports kink, antikink, and breather solutions. These solutions exhibit non-trivial scattering yet retain their shape, which made the model a cornerstone in the study of integrable systems [6, 50]. Therefore, this model is one of the most studied integrable models in the community. Similarly, it also has one of the first exact S-matrix solutions [7].

With the flat Minkowski metric, which has the minus sign convention for the time coordinate, the sine-Gordon model is described by the Lagrangian density

$$\mathcal{L}_{SG} = \frac{1}{2} (\partial \phi)^2 + \frac{m^2}{\beta^2} (\cos(\beta \phi) - 1) , \qquad (3.2)$$

which has the well-known classical solutions with the boundary conditions

$$\phi \to 0 \quad x \to -\infty, \qquad \phi \to \frac{2\pi}{\beta} \quad x \to \infty,$$
 (3.3)

and

$$\phi \to \frac{2\pi}{\beta} \quad x \to -\infty, \qquad \phi \to 0 \quad x \to \infty,$$
 (3.4)

that lead to soliton(s) and antisoliton( $\bar{s}$ ) solutions, respectively. There is a topological charge with spin zero

$$Q_0 = \frac{\beta}{2\pi} \int_{-\infty}^{\infty} \partial_x \phi dx \tag{3.5}$$

associated with s and  $\bar{s}$  solutions.  $Q_0$  corresponds to the conservation of the total number of solitons and equals +1 and -1 for s and  $\bar{s}$ , respectively. The model shows an infinite set of local conserved charges, both on the classical and on the quantum levels. The S-matrix of the quantum sine-Gordon model has been given in [7]. Since its quantum S-matrix solves the Yang-Baxter equation, it is therefore integrable, which is an equivalent way to realize that integrability survives on the quantum

level. The only non-diagonal part in the S-matrix

$$S_{SG}(\theta) = \begin{pmatrix} S(\theta) & & & \\ & S_T(\theta) & S_R(\theta) & & \\ & S_R(\theta) & S_T(\theta) & & \\ & & S(\theta) \end{pmatrix}$$
(3.6)

is where the total soliton number is equal to zero. In equation (3.6), we defined  $\theta = \theta_{12} \equiv \theta_1 - \theta_2$ , and the basis for the S-matrix as  $\{|s\rangle \otimes |s\rangle$ ,  $|s\rangle \otimes |\bar{s}\rangle$ ,  $|\bar{s}\rangle \otimes |s\rangle$ ,  $|\bar{s}\rangle \otimes |\bar{s}\rangle$ . Hence, we can write

$$A_s(\theta_1)A_s(\theta_2) = S(\theta)A_s(\theta_2)A_s(\theta_1) , \qquad (3.7)$$

$$A_s(\theta_1)A_{\bar{s}}(\theta_2) = S_T(\theta)A_{\bar{s}}(\theta_2)A_s(\theta_1) + S_R(\theta)A_s(\theta_2)A_{\bar{s}}(\theta_1) . \tag{3.8}$$

It can be clearly seen that  $S_T(\theta)$  stands for the transmission and  $S_R(\theta)$  stands for the reflection amplitudes. It is easy to check that they satisfy the unitarity condition

$$S(\theta)S(-\theta) = 1 , \qquad (3.9)$$

$$S_T(\theta)S_T(-\theta) + S_R(\theta)S_R(-\theta) = 1 , \qquad (3.10)$$

$$S_T(\theta)S_R(-\theta) + S_R(\theta)S_T(-\theta) = 0 , \qquad (3.11)$$

and the crossing symmetry

$$S(i\pi - \theta) = S_T(\theta) , \qquad (3.12)$$

$$S_R(i\pi - \theta) = S_R(\theta) . (3.13)$$

 $S_{SG}(\theta)$  amplitudes are explicitly given in [7] as the following.

$$S_T(\theta) = -\frac{i}{\pi} \sinh\left(\frac{8\pi}{\gamma}\theta\right) R(\theta) R(i\pi - \theta), \tag{3.14}$$

$$S_T(\theta) = -\frac{i}{\pi} \sinh\left(\frac{8\pi}{\gamma}\theta\right) R(\theta) R(i\pi - \theta), \qquad (3.14)$$

$$S_R(\theta) = \frac{1}{\pi} \sin\left(\frac{8\pi^2}{\gamma}\right) R(\theta) R(i\pi - \theta), \qquad (3.15)$$

$$S(i\pi - \theta) = S_T(\theta), \tag{3.16}$$

with

$$R(\theta) = \Gamma \left( 1 + i \frac{8\theta}{\gamma} \right) \prod_{l=1}^{\infty} \frac{\Gamma \left( 2l \frac{8\pi}{\gamma} + i \frac{8\theta}{\gamma} \right) \Gamma \left( 1 + 2l \frac{8\pi}{\gamma} + i \frac{8\theta}{\gamma} \right)}{\Gamma \left( (2l+1) \frac{8\pi}{\gamma} + i \frac{8\theta}{\gamma} \right) \Gamma \left( 1 + (2l-1) \frac{8\pi}{\gamma} + i \frac{8\theta}{\gamma} \right)}, \tag{3.17}$$

where  $\gamma = \beta^2 \left(1 - \frac{\beta^2}{8\pi}\right)^{-1}$ , and l is from  $-l\pi < \text{Im}(\theta) < (-l+1)\pi$ . These amplitudes also contain the information about the pole structure and the bound states which are outside the physical strip. We will now take a closer look at the pole structure inside the physical strip, which corresponds to l = 0, since we are interested in the physical spectrum.

It turns out that there is a family of solutions called breather solutions, which correspond to the bound states formed by s and  $\bar{s}$ . They have breather mass

$$M_k = 2M \sin \frac{\pi k}{h}$$
,  $k = 1, 2, \dots < \frac{8\pi}{\beta^2} - 1$  (3.18)

where  $h = \frac{16\pi}{\beta^2} \left(1 - \frac{\beta^2}{8\pi}\right)$  and M is the soliton mass. These solutions are located at the poles of the amplitudes

$$\theta = \left(1 - k\frac{2}{h}\right)\pi i, \quad k = 1, 2 \dots \quad \text{for } S_T(\theta), \tag{3.19}$$

$$\theta = k \frac{2}{h} \pi i, \quad k = 1, 2 \dots \quad \text{for } S(\theta), \tag{3.20}$$

$$\theta = \left(1 - k\frac{2}{h}\right)\pi i \quad \& \quad \theta = k\frac{2}{h}\pi i, \quad k = 1, 2 \dots \quad \text{for } S_R(\theta), \tag{3.21}$$

on the physical strip. These special points  $\theta = iu_{s\bar{s}}^b$  on the  $\theta$ -plane, where s and  $\bar{s}$  fuse into a breather b, defines the fusing angle  $u_{s\bar{s}}^b$  Fig.(2.6). The first breather's, corresponding to k = 1 in equation (3.18), scattering element can be given by

$$S_{bb}(\theta,\lambda) = \frac{\sinh\theta + i\sin(\gamma/8)}{\sinh\theta - i\sin(\gamma/8)},$$
(3.22)

where  $\gamma = \beta^2 \left(1 - \frac{\beta^2}{8\pi}\right)^{-1}$  and  $2m \cosh \theta = s - 2m^2$ , [7]. The equation (3.22) is a typical form of a CDD factor (named after Castillejo, Dalitz, and Dyson, [1]), which is an extra multiplicative factor in an S-matrix that is not determined by the unitarity, analyticity, and crossing symmetry alone. Although the symmetry properties of the

S-matrix remain the same under these factors, the new pole structure is immensely dissimilar. We can utilize these CDD factors to shift some poles outside or inside the physical strip. Hence, they lead to two distinct physical theories which have completely different particle spectrums while preserving the basic properties of an S-matrix.

#### 3.2 The Sausage Model

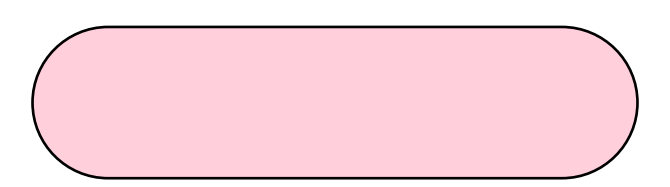


Figure 3.1: The deformed target space in the sausage model. For  $\nu \to 0$ , it approaches a sphere, and for large  $\nu$ , it becomes elongated like a cylinder in the family of  $SSM_{\nu}^{(\theta)}$  theories. (Color Code: Bologna Sausage #ffcfdc)

The sausage model is a two-dimensional quantum field theory that can be thought of as a smooth, integrable "squashing" of the familiar O(3) nonlinear sigma model Fig.(3.1). Therefore, let us first introduce the O(3) sigma model . It is described by the following action.

$$S_{O(3)} = \frac{1}{2g} \sum_{a=1}^{3} \int (\partial_{\mu} n_a)^2 d^2 x + i\Theta T , \qquad (3.23)$$

where  $n_a(x)$  are unit vector fields of O(3) with  $\sum_{a=0}^3 n_a^2 = 1$ ,  $0 \le \Theta < 2\pi$  is the topological angle, and T is the integer valued instanton charge

$$T = \frac{1}{8\pi} \int \sum_{abc} \epsilon^{abc} n_a \,\partial_{\mu} n_b \,\partial_{\nu} n_c \,\epsilon_{\mu\nu} \,\mathrm{d}^2 x \ . \tag{3.24}$$

We will follow the notation in [34] and call this field theory as  $SSM_0^{(\theta)}$  field theory. We will discuss the special points where the topological angle  $\Theta$  equals 0 and  $\pi$  only. These points are the two integrable points along the set of points. It is worth

noting that the on-mass-shell physics depends on  $\Theta$  values in general. Hence, even at this stage, we would expect the two theories will describe different physics at large distances. In particular,  $SSM_0^{(0)}$  is a massive theory with a finite correlation length, whereas  $SSM_0^{(\pi)}$  doesn't have a mass gap, and its correlation length is infinite in the IR limit. This scale invariance of the  $SSM_0^{(\pi)}$  at large distances is described by the  $SU(2) \times SU(2)$  WZW theory at level k = 1, a conformal field theory with a central charge c = 1 Fig.(3.2).

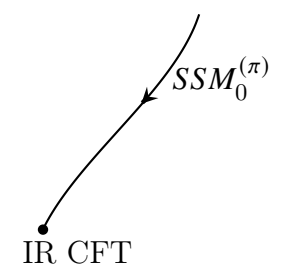


Figure 3.2: RG trajectory of the O(3) sigma model at  $\theta = \pi$ .

The particle spectrum of the  $SSM_0^{(0)}$  theory has three massive particles  $A_a$ , a = 1, 2, 3. The factorized scattering with respect to them is characterized by the two-particle S-matrix. In the non-commutative notation that we introduced in the section (2.2.1), we have

$$A_a(\theta_1)A_b(\theta_2) = S_{ab}^{cd}(\theta)A_d(\theta_2)A_c(\theta_1) , \qquad (3.25)$$

where  $\theta_1 > \theta_2$  and  $\theta = \theta_{12} = \theta_1 - \theta_2$ . This mapping between the incoming and the outgoing states can be written as

$$S(\theta)_{ab}^{cd} = S_0(\theta) (P_0)_{ab}^{cd} + S_1(\theta) (P_1)_{ab}^{cd} + S_2(\theta) (P_2)_{ab}^{cd} , \qquad (3.26)$$

where

$$(P_0)_{ab}^{cd} = \frac{1}{3}\delta_{ab}\delta_{cd} , \qquad (3.27)$$

$$(P_1)_{ab}^{cd} = \frac{1}{2} \delta_{ac} \delta_{bd} - \frac{1}{2} \delta_{ad} \delta_{bc} , \qquad (3.28)$$

$$(P_2)_{ab}^{cd} = \frac{1}{2}\delta_{ac}\delta_{bd} + \frac{1}{2}\delta_{ad}\delta_{bc} - \frac{1}{3}\delta_{ab}\delta_{cd}$$
(3.29)

are the projectors on the two-particle states with isospin 0, 1, and 2, respectively. The partial amplitudes are

$$S_0(\theta) = \frac{\theta + 2i\pi}{\theta - 2i\pi},\tag{3.30}$$

$$S_1(\theta) = \frac{(\theta - i\pi)(\theta + 2i\pi)}{(\theta + i\pi)(\theta - 2i\pi)},$$
(3.31)

$$S_2(\theta) = \frac{\theta - i\pi}{\theta + i\pi} \ . \tag{3.32}$$

The UV central charge is shown to be  $c_{UV} = 2$  as one might expect [23, 24, 33].

On the other hand, the particle spectrum of the  $SSM_0^{(\pi)}$  theory has two massless particles called left-movers  $L_{\sigma}(\theta)$  and right-movers  $R_{\sigma}(\theta)$ , which are SU(2)-doublets with  $\sigma = \pm$ . The corresponding S-matrix elements are given by

$$A_{R_{\sigma_1}}(\theta_1)A_{R_{\sigma_2}}(\theta_2) = S^{(RR)}_{\sigma_1\sigma_2}^{\sigma_1'\sigma_2'}(\theta)A_{R_{\sigma_2'}}(\theta_2)A_{R_{\sigma_1'}}(\theta_1) , \qquad (3.33)$$

$$A_{L_{\sigma_{1}}}(\theta_{1})A_{L_{\sigma_{2}}}(\theta_{2}) = S^{(LL)}_{\sigma_{1}\sigma_{2}}^{\sigma_{1}'\sigma_{2}'}(\theta)A_{L_{\sigma_{2}'}}(\theta_{2})A_{L_{\sigma_{1}'}}(\theta_{1}) , \qquad (3.34)$$

$$A_{R_{\sigma_{1}}}(\theta_{1})A_{L_{\sigma_{2}}}(\theta_{2}) = S^{(RL)}_{\sigma_{1}\sigma_{2}}^{\sigma'_{1}\sigma'_{2}}(\theta)A_{L_{\sigma'_{2}}}(\theta_{2})A_{R_{\sigma'_{1}}}(\theta_{1}) , \qquad (3.35)$$

where

$$S^{(LL)}{\sigma_{1}\sigma_{2}'\sigma_{2}'(\theta)} = S^{(RR)}{\sigma_{1}\sigma_{2}'\sigma_{2}'(\theta)} = S^{(RL)}{\sigma_{1}\sigma_{2}'\sigma_{2}'(\theta)} = \frac{\Gamma\left(\frac{1}{2} + \frac{\theta}{2i\pi}\right)\Gamma\left(-\frac{\theta}{2i\pi}\right)}{\Gamma\left(\frac{1}{2} - \frac{\theta}{2i\pi}\right)\Gamma\left(\frac{\theta}{2i\pi}\right)} \left(\frac{\theta\delta_{\sigma_{1}}^{\sigma_{1}'}\delta_{\sigma_{2}}^{\sigma_{2}'} - i\pi\delta_{\sigma_{1}}^{\sigma_{2}'}\delta_{\sigma_{2}}^{\sigma_{1}'}}{\theta - i\pi}\right). \tag{3.36}$$

For  $SSM_0^{(\pi)}$  theory, it is shown that the theory interpolates between two CFT's with  $c_{UV} = 2$  and  $c_{IR} = 1$  [33]. It can also be written as the summation of the projectors on the two-particle states with the corresponding partial amplitudes, in fact, the gamma function in front of the parentheses in the (3.36) is the partial amplitude of the isospin-1 channel.

Now, let us study the sausage model as a deformation of the two types of O(3) nonlinear sigma model we introduced. We will refer to these factorized scattering theories as the sausage scattering theories  $(SST_{\lambda}^{(\pm)})$ . The (+) and (-) cases have the same particle spectrum as  $SSM_0^{(0)}$  and  $SSM_0^{(\pi)}$ , respectively.

Let us begin with  $SST_{\lambda}^{(+)}$ , first studied in [13]. Here, the triplet (+,0,-) represents three massive particles. Their scattering process results in the following amplitudes.

$$S_{++}^{++}(\theta) = S_{+-}^{+-}(i\pi - \theta) = \frac{\sinh(\lambda(\theta - i\pi))}{\sinh(\lambda(\theta + i\pi))},$$
(3.37)

$$S_{+0}^{0+}(\theta) = S_{+-}^{00}(i\pi - \theta) = \frac{-i\sin(2\pi\lambda)}{\sinh(\lambda(\theta - 2i\pi))} S_{++}^{++}(\theta), \tag{3.38}$$

$$S_{+0}^{+0}(\theta) = \frac{\sinh(\lambda \theta)}{\sinh(\lambda(\theta - 2i\pi))} S_{++}^{++}(\theta), \tag{3.39}$$

$$S_{+-}^{-+}(\theta) = -\frac{\sin(\pi\lambda)\sin(2\pi\lambda)}{\sinh(\lambda(\theta - 2i\pi))\sinh(\lambda(\theta + i\pi))},$$
(3.40)

$$S_{00}^{00}(\theta) = S_{+0}^{+0}(\theta) + S_{-+}^{+-}(\theta). \tag{3.41}$$

In the limit  $\lambda \to 0$ , the amplitudes (3.37)-(3.41) of  $SST_{\lambda}^{(+)}$  reduce to the amplitudes (3.26)-(3.32) of  $SSM_0^{(0)}$ . In the limit  $\lambda \to 1/2$ , the theory becomes a free theory with ±1 in the diagonal S-matrix representing two massive fermionic particles and one massive bosonic particle. When  $\lambda > 1/2$ , the theory has bound states and therefore a more complicated particle spectrum, which requires more complicated tools to study due to its pole structure.

Next, the  $SST_{\lambda}^{(-)}$  theory contains two massless particles, which are the same as we mentioned above as left-movers and right-movers. They are written as the doublets (+, -). Its S-matrix follows as

$$S^{(LL)}_{++}^{++}(\theta) = S^{(LL)}_{--}^{--}(\theta) = U_0(\theta),$$
 (3.42)

$$S^{(LL)^{+-}}_{+-}(\theta) = S^{(LL)^{-+}}_{-+}(\theta) = -\frac{\sinh(\lambda\theta/(1-\lambda))}{\sinh(\lambda(\theta-i\pi)/(1-\lambda))} U_0(\theta), \qquad (3.43)$$

$$S^{(LL)^{+-}}_{-+}(\theta) = S^{(LL)^{-+}}_{+-}(\theta) = -i\frac{\sin(\pi\lambda/(1-\lambda))}{\sinh(\lambda(\theta-i\pi)/(1-\lambda))} U_0(\theta), \qquad (3.44)$$

$$S^{(LL)^{+-}}_{-+}(\theta) = S^{(LL)^{-+}}_{+-}(\theta) = -i \frac{\sin(\pi\lambda/(1-\lambda))}{\sinh(\lambda(\theta-i\pi)/(1-\lambda))} U_0(\theta), \tag{3.44}$$

$$S^{(RR)}_{\sigma_1\sigma_2}^{\sigma_1'\sigma_2'}(\theta) = S^{(LL)}_{\sigma_1\sigma_2}^{\sigma_1'\sigma_2'}(\theta), \tag{3.45}$$

$$S^{(RL)}_{\sigma_1\sigma_2}^{\sigma_1'\sigma_2'}(\theta) = S^{(LL)}_{\sigma_1\sigma_2}^{\sigma_1'\sigma_2'}(\theta)$$

$$\tag{3.46}$$

where

$$U_0(\theta) = -\exp\left[i\int_0^\infty \frac{\sinh\left((1-2\lambda)\pi\omega/(2\lambda)\right)\sin(\omega\theta)}{\cosh(\pi\omega/2)\sinh\left((1-\lambda)\pi\omega/(2\lambda)\right)}\frac{d\omega}{\omega}\right]. \tag{3.47}$$

Here, we assumed  $S^{(RL)}_{\sigma_1\sigma_2}^{\sigma_1'\sigma_2'}(\theta) = S^{(LL)}_{\sigma_1\sigma_2}^{\sigma_1'\sigma_2'}(\theta-\theta_0) = S^{(RR)}_{\sigma_1\sigma_2}^{\sigma_1'\sigma_2'}(\theta-\theta_0)$  for an arbitrary real shift  $\theta_0$  and set it to zero. These amplitudes match the Sine-Gordon model's amplitudes (3.14)-(3.17) in the integral representation up to a redefinition of the couplings in the action.

In the limit,  $\lambda \to 0$ , we obtain the  $SSM_0^{(\pi)}$  FST (3.36) back. In the limit  $\lambda \to 1/2$ , the theory seems to contain free massless fermions with an S-matrix equals to  $-\mathbb{I}$ . However, there is a pole entering the s-channel cut as  $\lambda$  approaches 1/2, which makes a neutral boson  $B_0$  formed by  $R_+L_-$  or  $R_-L_+$ , a stable particle in the spectrum. Hence, the full spectrum of  $SST_{1/2}^{(-)}$  has two complex, massless, and charged fermions  $R_\pm$  and  $L_\pm$  and one neutral and massive boson  $B_0$ . It is a free field theory with  $c_{UV}=2$ , as one can expect. When  $\lambda > 1/2$ , poles begin to enter the physical strip. This makes the theory extremely complicated since the bootstrap program is a challenging process in general. Therefore, we strictly take  $SST_{\lambda}^{(\pm)}$  theories with  $0 \le \lambda \le 1/2$  into account throughout this paper.

# 3.3 Exact Scattering Processes of The Higher-spin Particles

Recent research studies provided an S-matrix construction for particles with general spins [54]. They constructed and studied a new class of exact factorized scattering theories, which generalize the sine-Gordon and sausage models to higher-spin representations of the quantum group  $\mathcal{U}_q(su(2))$ . These models come equipped with minimal exact S-matrices, meaning no additional CDD factors, that satisfy unitarity, crossing symmetry, and the Yang-Baxter equation. Building upon these S-matrices, the authors derive corresponding TBA equations and analyze the free energies. What they find is striking: for spins greater than or equal to 3/2, the free energy develops singularities reminiscent of the Hagedorn transition. While the critical scale at which the singularity appears depends on both the spin and the coupling constant, the critical exponent associated with the divergence is found to

be universal, close to 1/2, suggesting a square-root type singularity.

This issue has been highlighted recently in studies of  $T\bar{T}$  deformations of integrable QFTs. Such deformations effectively add CDD factors to the S-matrix [46], and in most cases, they generate Hagedorn-like singularities in the free energy. Although some fine-tuned cases can avoid the singularity and flow to ultraviolet complete theories [46, 52], the general expectation is that irrelevant deformations trigger these singular behaviors. Yet, this leaves open the possibility that singularities may be intrinsic to the original undeformed scattering theories themselves.

#### 3.3.1 The General S-matrix Construction

Let us introduce the  $\mathfrak{su}_2$  algebra generated by  $\mathbb{J}_{\pm}$ ,  $\mathbb{J}_3$ , which has the following commutation relations and the Casimir operator  $\mathbb{Q}$ .

$$[\mathbb{J}_{\pm}, \mathbb{J}_3] = \pm \mathbb{J}_{\pm} \quad , \quad [\mathbb{J}_{+}, \mathbb{J}_{-}] = 2\mathbb{J}_3$$
 (3.48)

$$\mathbb{Q} = \mathbb{J}^2 = \frac{\mathbb{J}_+ \mathbb{J}_- + \mathbb{J}_- \mathbb{J}_+}{2} + \mathbb{J}_3^2$$
 (3.49)

Now, consider a two-particle S-matrix  $S(\theta)$  of an FST between particles that belong to the spin s irreducible representation of the  $\mathfrak{su}_2$ . We can decompose the S-matrix similar to Eq.(3.26) as

$$S(\theta) = P \sum_{J=0}^{2s} f^{[J]}(\theta) \, \mathbb{P}^{[J]}, \tag{3.50}$$

where P is the permutation matrix,  $\mathbb{P}^{[J]}$  the projector on the spin-J representation, and  $f^{[J]}(\theta)$  are the scalar functions

$$f^{[J]}(\theta) = \prod_{k=1}^{J} \frac{i\pi k - \theta}{i\pi k + \theta}$$
 (3.51)

to be determined by the Yang-Baxter equation up to an overall function. The matrix elements of the projectors are given by the Clebsch-Gordan coefficients as

$$\mathbb{P}^{[J]_{m_1m_2}^{m'_1m'_2}} = \sum_{M=-J}^{J} \langle s, m'_1; s, m'_2 | J, M \rangle \langle J, M | s, m_1; s, m_2 \rangle.$$
 (3.52)

They also satisfy

$$\sum_{I=0}^{2s} \mathbb{P}^{[J]} = \mathbb{I} , \quad \text{and} \quad \left(\mathbb{P}^{[J]}\right)^2 = \mathbb{P}^{[J]}. \tag{3.53}$$

Such S-matrices have been known and studied for some time [36]. We will focus on the deformations of the S-matrices of this kind to generalize them to arbitrary spins.

Our deformation parameter  $q \in \mathbb{C}$  belongs to the quantum group symmetry algebra  $\mathcal{U}_q(\mathfrak{su}_2)$ , which is generated by  $\mathbb{J}_{\pm}$ ,  $q^{\pm \mathbb{J}_3}$ , with the following commutation relations and the Casimir operator  $\mathbb{Q}$ .

$$[\mathbb{J}_{\pm}, \mathbb{J}_3] = \pm \mathbb{J}_{\pm}, \qquad [\mathbb{J}_{+}, \mathbb{J}_{-}] = [2\mathbb{J}_3]$$
 (3.54)

$$\mathbb{Q} = \mathbb{J}_{+}\mathbb{J}_{-} + \left[\mathbb{J}_{3} - \frac{1}{2}\right] = \mathbb{J}_{-}\mathbb{J}_{+} + \left[\mathbb{J}_{3} + \frac{1}{2}\right], \tag{3.55}$$

where

$$[\lambda] \equiv \frac{q^{\lambda/2} - q^{-\lambda/2}}{q^{1/2} - q^{-1/2}} \ . \tag{3.56}$$

An eigenvector  $|J, M\rangle$  of the operators  $\mathbb{Q}$  and  $\mathbb{J}_3$  reads

$$\mathbb{Q}|J,M\rangle = \left[J + \frac{1}{2}\right]|J,M\rangle \qquad , \qquad \mathbb{J}_3|J,M\rangle = M|J,M\rangle . \tag{3.57}$$

It is worth to mention the definition of a q-factorial for future use at this point. It is defined for non-negative integer n as

$$[n]! = [n][n-1]\cdots[1], \quad [0]! = 1, \quad [-n]! = \infty.$$
 (3.58)

By comparison with the equation (3.50), the q-version of the S-matrix of the asymptotic particles is given by

$$S(\theta) = \sigma \left( P \sum_{J=0}^{2s} f_q^{[J]}(\theta) \, \mathbb{P}_q^{[J]} \right) \sigma^{-1} , \qquad (3.59)$$

where  $\mathbb{P}_q^{[J]}$  are q-deformed projectors, P is a permutation matrix,  $\sigma$  is the gauge transformation

$$\sigma = q^{\mathbb{I}_3 \,\theta_1/2\pi i} \otimes q^{\mathbb{I}_3 \,\theta_2/2\pi i},\tag{3.60}$$

and  $f_q^{[J]}(\theta)$  are the trigonometric scalar functions

$$f_q^{[J]}(\theta) = S_0(\theta) \prod_{k=1}^{J} \frac{\sinh[\gamma(i\pi k - \theta)]}{\sinh[\gamma(i\pi k + \theta)]}, \qquad J = 0, 1, \dots, 2s$$
(3.61)

with

$$S_{0}(\theta) = -\prod_{k=1}^{2s} \left[ \frac{\sinh \left[ \gamma(i\pi k + \theta) \right]}{\sinh \left[ \gamma(i\pi k - \theta) \right]} \left( \prod_{l=1}^{\infty} \frac{\sinh \left[ \gamma(i\pi(k+l) - \theta) \right] \sinh \left[ \gamma(i\pi(k-l) - \theta) \right]}{\sinh \left[ \gamma(i\pi(k+l) + \theta) \right] \sinh \left[ \gamma(i\pi(k-l) + \theta) \right]} \right) \right], \tag{3.62}$$

where we bring in the coupling constant  $\gamma$  via

$$q = e^{2\pi i \gamma}. (3.63)$$

The scalar prefactor  $S(\theta)$  is determined by the unitarity and crossing symmetry constraints

$$S_0(\theta)S_0(-\theta) = 1$$
 and  $S_0(i\pi - \theta) = \prod_{k=1}^{2s} \frac{\sinh \left[\gamma(i(k+1)\pi - \theta)\right]}{\sinh \left[\gamma(ik\pi + \theta)\right]} S_0(\theta)$ , (3.64)

respectively.

Hitherto, we were able to build the projectors  $\mathbb{P}^{[J]}$  in equation (3.52) with Clebsch-Gordan coefficients. Comparably, we will assemble the q-deformed projectors  $\mathbb{P}_q^{[J]}$  by using quantum Clebsch-Gordan coefficients(qCGs), studied in the early 1990's [26, 29, 31]

$$\langle s, m_1; s, m_2 | J, M \rangle_q = f(J) \cdot q^{(2s-J)(2s+J+1)/4+s(m_2-m_1)/2}$$

$$\times \{ [s+m_1]![s-m_1]![s+m_2]![s-m_2]![J+M]![J-M]! \}^{1/2} \sum_{\nu \geq 0} (-1)^{\nu} \frac{q^{-\nu(2s+J+1)/2}}{\mathcal{D}_{\nu}},$$

where

$$f(J) = \left\{ \frac{[2J+1]([J]!)^2[2s-J]!}{[2s+J+1]!} \right\}^{1/2},$$

$$\mathcal{D}_{\nu} = [\nu]![2s-J-\nu]![s-m_1-\nu]![s+m_2-\nu]![J-s+m_1+\nu]![J-s-m_2+\nu]!.$$
(3.66)

Therefore, the q-deformed projectors read

$$\mathbb{P}_{q \ m_1 m_2}^{[J]m_1'm_2'} = \sum_{M=-J}^{J} \langle s, m_1'; s, m_2' | J, M \rangle_q \langle J, M | s, m_1; s, m_2 \rangle_q . \tag{3.67}$$

The particles are a part of the spin s representation of  $\mathcal{U}_q(\mathfrak{su}_2)$ .

The authors in [54] were able to recast the S-matrix (3.59) by introducing a prefactor in the integral representation

$$S_{ss}^{ss}(\theta) = -\exp \int_{-\infty}^{\infty} \frac{dk}{k} \frac{\sinh(\pi k s) \sinh \pi k (s - \frac{1}{2\gamma})}{\sinh \frac{\pi k}{2\gamma} \sinh \pi k} e^{ik\theta}, \tag{3.68}$$

which has the same form for all integer and half-integer spin values s. The S-matrix with this prefactor is described as

$$S(\theta) = S_{ss}^{ss}(\theta) \cdot S_{\text{mat}}(\theta), \tag{3.69}$$

where

$$S_{\text{mat}}(\theta) \equiv \sigma \left( P \sum_{l=0}^{2s} \left[ \prod_{k=l+1}^{2s} \frac{\sinh \left[ \gamma(ik\pi + \theta) \right]}{\sinh \left[ \gamma(ik\pi - \theta) \right]} \right] \mathbb{P}_q^{[J]} \right) \sigma^{-1}.$$
 (3.70)

It is discussed in [54] that the scattering theory becomes free at  $\gamma = \frac{1}{2s}$ 

$$S_{ss}^{ss}(\theta) = -1$$
 for  $\gamma = \frac{1}{2s}$  (3.71)

The physical strip is free from poles for the values  $0 \le \gamma \le \frac{1}{2s}$ , which is called the repulsive regime. The region  $\gamma > \frac{1}{2s}$  is known as the attractive regime, where the theory begins to contain bound states. Before considering the spin 3/2 case, let us briefly mention the results for the spin 1/2 and the spin 1 cases when  $\gamma$  tends to  $\frac{1}{2s}$ .

For s = 1/2, we arrive at the S-matrix of the sine-Gordon model by following the above procedure after choosing a suitable permutation matrix. Here, our q-deformed projectors are

$$\mathbb{P}_{q}^{[0]}|_{\gamma=1} = \begin{pmatrix} 0 & 0 & 0 & 0 \\ 0 & \frac{1}{2} & -\frac{1}{2} & 0 \\ 0 & -\frac{1}{2} & \frac{1}{2} & 0 \\ 0 & 0 & 0 & 0 \end{pmatrix}, \tag{3.72}$$

$$\mathbb{P}_{q}^{[1]}|_{\gamma=1} = \begin{pmatrix} 1 & 0 & 0 & 0 \\ 0 & \frac{1}{2} & \frac{1}{2} & 0 \\ 0 & 0 & 0 & 1 \end{pmatrix}. \tag{3.73}$$

$$\mathbb{P}_{q}^{[1]}|_{\gamma=1} = \begin{pmatrix}
1 & 0 & 0 & 0 \\
0 & \frac{1}{2} & \frac{1}{2} & 0 \\
0 & \frac{1}{2} & \frac{1}{2} & 0 \\
0 & 0 & 0 & 1
\end{pmatrix}.$$
(3.73)

Let us present the S-matrix, constructed from the q-deformed projectors above, via (3.69) and (3.70). In the free point, where  $\gamma = \frac{1}{2s} = 1$ , the S-matrix is given by

$$S|_{\gamma=1} = \begin{pmatrix} -1 & 0 & 0 & 0 \\ 0 & -1 & 0 & 0 \\ 0 & 0 & -1 & 0 \\ 0 & 0 & 0 & -1 \end{pmatrix}.$$
 (3.74)

The exchange rules that we can derive from this S-matrix imply that the particles in the spectrum should obey only the fermionic statistics. We have two free fermions.

For s = 1, by using qCGs (3.65), q-deformed projectors (3.67) becomes

$$\mathbb{P}_{q}^{[0]}|_{\gamma=\frac{1}{2}} = \begin{pmatrix}
0 & 0 & 0 & 0 & 0 & 0 & 0 & 0 & 0 & 0 \\
0 & 0 & 0 & 0 & 0 & 0 & 0 & 0 & 0 & 0 \\
0 & 0 & \frac{1}{3} & 0 & -\frac{1}{3} & 0 & \frac{1}{3} & 0 & 0 & 0 \\
0 & 0 & -\frac{1}{3} & 0 & \frac{1}{3} & 0 & -\frac{1}{3} & 0 & 0 & 0 \\
0 & 0 & 0 & 0 & 0 & 0 & 0 & 0 & 0 & 0 \\
0 & 0 & \frac{1}{3} & 0 & -\frac{1}{3} & 0 & \frac{1}{3} & 0 & 0 & 0 \\
0 & 0 & 0 & 0 & 0 & 0 & 0 & 0 & 0 & 0 \\
0 & 0 & 0 & 0 & 0 & 0 & 0 & 0 & 0 & 0
\end{pmatrix} (3.75)$$

The S-matrix, constructed from these q-deformed projectors, results in the same S-matrix (3.37)-(3.41) of  $SST_{\lambda}^{(+)}$  after a suitable change of basis. In the free point, where  $\gamma = \frac{1}{2s} = 1/2$ , the S-matrix is given by

which corresponds to the S-matrix of the  $SST_{\frac{1}{2}}^{(+)}$ . Therefore, it also has the same particle spectrum as well. We have two free fermionic particles  $A_{\pm}$  and one free bosonic particle  $A_0$ . If we interpret  $A_{\pm}$  as components of a free Dirac fermion and  $A_0$  as a free boson on the fixed point, we can immediately see how their contribution adds up to  $c_{UV} = 2$ . In this case, the exchange rules that we can derive from this S-matrix bring about not only fermionic but also bosonic statistics between particles.

Similarly, the S-matrix of  $SST_{\lambda}^{(-)}$  (3.42)-(3.47) can also be decomposed into irreducible spin-J sectors by using the q-deformed projectors, which allows us to compute the S-matrix as a sum of the q-projectors. In fact, its S-matrix is the sine-Gordon model's S-matrix in the integral representation.

## 3.3.2 The Spin 3/2 Case

For s = 3/2, the authors of [54] stated that, with the above formulation, the S-matrix for this case is given by

$$S_{11}^{11} = 1, \quad S_{12}^{12} = \frac{(0)}{(3)}, \quad S_{12}^{21} = \frac{s_3}{(3)}, \quad S_{13}^{13} = \frac{(0)(-1)}{(2)(3)}, \quad S_{13}^{22} = \frac{s_2\sqrt{s_3/s_1(0)}}{(2)(3)}, \quad (3.79)$$

$$S_{13}^{31} = \frac{(s_1s_4 + 2s_2)(0)}{(2)(3)}, \quad S_{22}^{22} = \frac{f_1}{(2)(3)}, \quad S_{14}^{14} = \frac{(0)(-1)(-2)}{(1)(2)(3)}, \quad S_{14}^{23} = \frac{s_3(0)(-1)}{(1)(2)(3)}, \quad S_{14}^{23} = \frac{s_2s_3(0)}{(1)(2)(3)}, \quad S_{14}^{23} = \frac{s_2s_3(0)}{(1)(2$$

where

$$s_n \equiv 2\sinh(in\pi\gamma),\tag{3.80}$$

$$(n) \equiv 2\sinh\left[\gamma(\theta - i\pi n)\right],\tag{3.81}$$

$$f_1 = 2\cosh\left[\gamma(2\theta - i\pi)\right] + \frac{s_{10}}{s_5} - 2\frac{s_2}{s_1},\tag{3.82}$$

$$f_2 = 2\frac{s_2}{s_1} \cosh\left[\gamma(2\theta - i\pi)\right] + s_2^2 - 2s_1^2 - 4. \tag{3.83}$$

We can determine all of the matrix elements by using the usual charge conjugation, parity, and time reversal symmetry of an S-matrix. The indices i, j, k, l of  $S_{ij}^{kl}$  in (3.79) take values from 1, 2, 3, 4, which represent the four particles  $A_m$  with m = -3/2, -1/2, 1/2, 3/2. They also satisfy  $\bar{A}_m = A_{-m}$  i.e.  $\bar{1} = 4$  and  $\bar{2} = 3$ . These matrix elements should be multiplied by the integral representation of the prefactor in the equation (3.68). Note that qCG coefficients in (3.65) are divergent for this case, therefore, one has to consult the [31] to construct the q-projectors. Let us have a look at the special point which corresponds to  $\gamma = \frac{1}{2s} = \frac{1}{3}$ . The prefactor  $S_{ss}^{ss}(\theta) = S_{ss}^{ss}|_{\gamma=\frac{1}{3}} = -1$  as normal for all  $\gamma = \frac{1}{2s}$ . Hence, the S-matrix becomes

where

$$A(\theta) = \frac{-2\sqrt{3} + 3i}{\sqrt{3}\cosh\left(\frac{\theta}{3}\right) - i\sinh\left(\frac{\theta}{3}\right)},\tag{3.85}$$

$$B(\theta) = \frac{-3\cosh\left(\frac{\theta}{3}\right) - i\sqrt{3}\sinh\left(\frac{\theta}{3}\right)}{2\cosh\left(\frac{2\theta}{3}\right) + 1},\tag{3.86}$$

$$A(\theta) = \frac{-2\sqrt{3} + 3i}{\sqrt{3}\cosh\left(\frac{\theta}{3}\right) - i\sinh\left(\frac{\theta}{3}\right)},$$

$$B(\theta) = \frac{-3\cosh\left(\frac{\theta}{3}\right) - i\sqrt{3}\sinh\left(\frac{\theta}{3}\right)}{2\cosh\left(\frac{2\theta}{3}\right) + 1},$$

$$C(\theta) = \frac{\sqrt{3}\cosh\left(\frac{\theta}{3}\right) + i\sinh\left(\frac{\theta}{3}\right)}{\sqrt{3}\cosh\left(\frac{\theta}{3}\right) - i\sinh\left(\frac{\theta}{3}\right)},$$

$$D(\theta) = \frac{1 - 2\sin\left(\frac{\pi}{6} - \frac{2i\theta}{3}\right)}{2\cosh\left(\frac{2\theta}{3}\right) + 1}.$$
(3.85)

$$D(\theta) = \frac{1 - 2\sin\left(\frac{\pi}{6} - \frac{2i\theta}{3}\right)}{2\cosh\left(\frac{2\theta}{3}\right) + 1}.$$
(3.88)

Interestingly, this special point does not seem like a free point as opposed to the s = 1/2 and s = 1 cases. Our S-matrix depends on the rapidity  $\theta$ , implying that there are some interactions.

A recent study suggests that this S-matrix is a Zamolodchikov-Faddeev(ZF) S-matrix, which appears in the ZF algebra, and has a nontrivial braiding statistics since it is rapidity-dependent. It is related to the physical S-matrix  $\mathbb S$  by a multiplication of the  $\mathcal R$ -matrix [56].

The equal rapidity limit  $\theta \to 0$  of this S-matrix leads to the following.

When 
$$\theta \to 0$$
,  $A(\theta) \to -2 + i\sqrt{3}$ ,  $B(\theta) \to -1$ ,  $C(\theta) \to 1$ ,  $D(\theta) \to 0$  (3.89)

After acting with a suitable permutation matrix, which exchanges the 7th and 10th row, the S-matrix has the following transmission and reflection amplitudes.

$$S_{ii}^{ij} = \pm 1 \tag{3.90}$$

$$S_{13}^{31} = S_{31}^{13} = S_{24}^{42} = S_{42}^{24} = -2 + i\sqrt{3}$$
(3.91)

The asymptotic limit  $\theta \to \infty$  leads to the following amplitudes.

When 
$$\theta \to \infty$$
,  $A(\theta) \& B(\theta) \to 0$ ,  $C(\theta) \to \frac{\left(1 + i\sqrt{3}\right)}{2}$ ,  $D(\theta) \to \frac{\left(-1 + i\sqrt{3}\right)}{2}$  (3.92)

When 
$$\theta \to -\infty$$
,  $A(\theta) \& B(\theta) \to 0$ ,  $C(\theta) \to \frac{\left(1 - i\sqrt{3}\right)}{2}$ ,  $D(\theta) \to \frac{\left(-1 - i\sqrt{3}\right)}{2}$  (3.93)

In this limit, the S-matrix does not become trivial, which suggests that one usually needs to adjust the crossing relations. To do so, one has to find the  $\mathcal{R}$ -matrix to determine the modified crossing equations.

In the notation of [56], it can be found by this asymptotic  $\theta \to \infty$  limit by assuming it is given as

$$\mathcal{R}_{12} = R_{12}u(\theta_{12}) + R_{21}^{-1}u(\theta_{21}) , \qquad (3.94)$$

where  $u(\theta)$  is the Heaviside function, whereas the  $R_{12}$  and  $R_{21}^{-1}$  are constant unitary matrices which satisfy the YBE. They usually do not satisfy the braiding unitarity  $R_{12} \neq R_{21}^{-1}$ . Then, we would say

$$S_{12}(\theta) \xrightarrow{\theta \to \infty} R_{12}, \quad S_{12}(-\theta) \xrightarrow{\theta \to \infty} (R_{21})^{-1}.$$
 (3.95)

In our case, we have

$$S_{12} \xrightarrow{\theta \to \infty} \mathcal{R}_{12}$$
, (3.96)

where we used (3.95) and the fact that  $\theta_1 > \theta_2$ . Now, one can consider the S-matrix (3.84) along with (3.92) as a diagonal  $\mathcal{R}$ -matrix. In our case, it has the form

$$\mathcal{R}_{AB}^{CD} = \delta_A^C \delta_B^D e^{-2\pi i \, s_{AB}} \,, \tag{3.97}$$

where  $s_{AB} = s_{BA}$  is a real number in Mod(1). The braiding factors  $s_{AB}$  of out S-matrix are given as

$$s_{11} = s_{13} = s_{24} = s_{31} = s_{42} = s_{44} = \frac{1}{2},$$
  $s_{22} = s_{33} = \frac{5}{6},$  (3.98)  
 $s_{12} = s_{14} = s_{21} = s_{34} = s_{41} = s_{43} = 0,$   $s_{23} = s_{32} = \frac{2}{3}.$  (3.99)

$$s_{12} = s_{14} = s_{21} = s_{34} = s_{41} = s_{43} = 0,$$
  $s_{23} = s_{32} = \frac{2}{3}.$  (3.99)

It would be interesting to see where these braiding factors lead to when they are applied to the relations and ideas in [56]. Here, we exclude this possibility because it is outside the scope of this thesis.

We can see the plots of the S-matrix amplitudes, which depend on rapidity in Fig. (3.3) and Fig. (3.4). The plots show how the S-matrix (3.84) becomes diagonal and constant for large  $\theta$  values.

However, we observe that the consistency for unitarity

$$S(\theta)S(-\theta) = \mathbb{I} \tag{3.100}$$

is not satisfied in  $\theta \to 0$  limit,  $S(0)S(0) \neq \mathbb{I}$ , whereas it is satisfied in the  $\theta \to \infty$ limit,  $S(\infty)S(-\infty) = \mathbb{I}$ . We can see the plot of the matrix elements of  $S(\theta)S(-\theta)$  in Fig. (3.8) and Fig. (3.9) to see how it shifts from non-unitary to unitary for large  $\theta$ values.

Furthermore, we can obtain a diagonal S-matrix (3.101) by picking a suitable particle basis, where the new particles will be represented as a combination of the particles in the current spectrum. The diagonal S-matrix becomes the following.

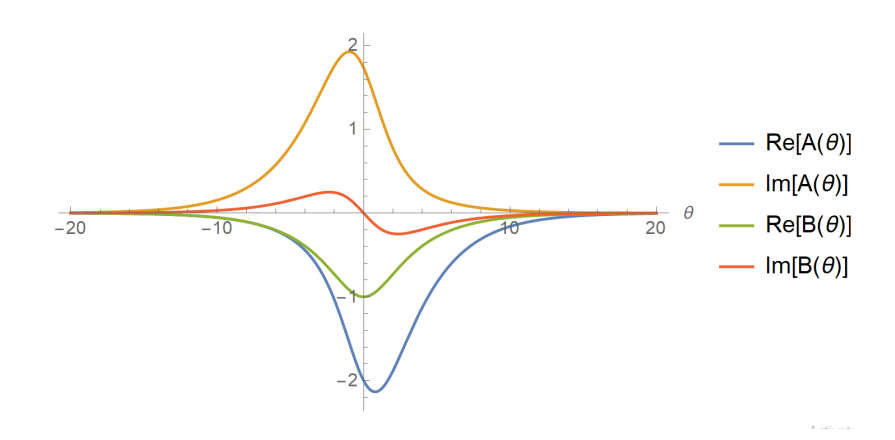


Figure 3.3: The  $\theta$  plot for the rapidity-dependent non-diagonal elements of the S-matrix (3.84).

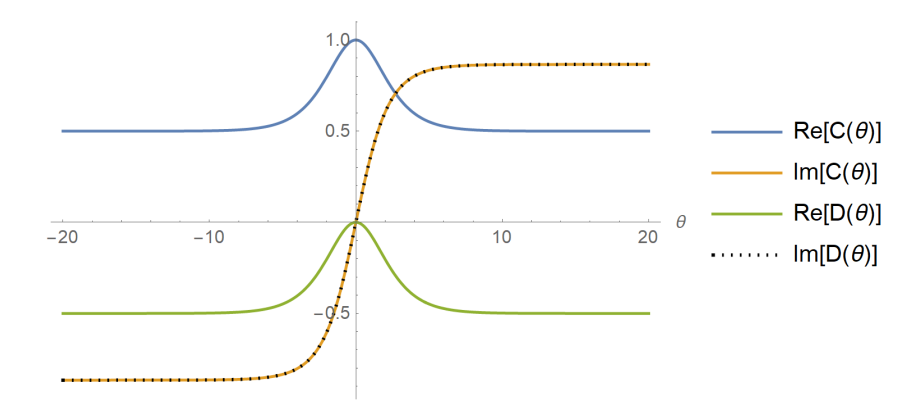


Figure 3.4: The  $\theta$  plot for the rapidity-dependent diagonal elements of the S-matrix (3.84).

where

$$A_1'(\theta) = -A(\theta) - 1 \tag{3.102}$$

$$A_2'(\theta) = A(\theta) - 1 \tag{3.103}$$

$$D_1'(\theta) = D(\theta) - B(\theta) \tag{3.104}$$

$$D_2'(\theta) = D(\theta) + B(\theta) \tag{3.105}$$

In the diagonal S-matrix, we can clearly see the braiding statistics between particles. It is worth mentioning that we have full control over the alignment of the elements(eigenvalues) on the diagonal since we can change their order by changing the order of the eigenvectors.

The equal rapidity limit  $\theta \to 0$  leads to the following amplitudes.

When 
$$\theta \to 0$$
,  $A_1'(\theta) \to 1 - i\sqrt{3}$ ,  $A_2'(\theta) \to -3 + i\sqrt{3}$ ,  $D_1'(\theta) \to 1$ ,  $D_2'(\theta) \to -1$  (3.106)

We can plot the behaviour of  $D'_1(\theta)$  and  $D'_2(\theta)$  as in the Fig.(3.5).

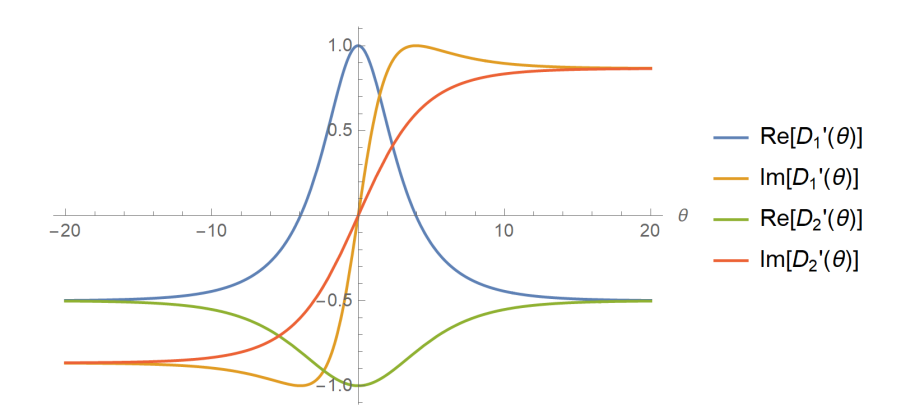


Figure 3.5: The  $\theta$  plot for the  $D_1'(\theta)$  and  $D_2'(\theta)$ .

The asymptotic limit  $\theta \to \infty$  leads to the amplitudes

When 
$$\theta \to \infty$$
,  $A'_1(\theta) \& A'_2(\theta) \to -1$ ,  $D'_1(\theta) \& D'_2(\theta) \to \frac{\left(-1 + i\sqrt{3}\right)}{2}$ , (3.107)  
When  $\theta \to -\infty$ ,  $A'_1(\theta) \& A'_2(\theta) \to -1$ ,  $D'_1(\theta) \& D'_2(\theta) \to \frac{\left(-1 - i\sqrt{3}\right)}{2}$ , (3.108)

together with the  $C(\theta \to \pm \infty)$  amplitudes already given above. In the trivial scattering limit, S-matrices are the same  $S|_{\gamma=\frac{1}{3}}(\theta \to \pm \infty) = S|_{\gamma=\frac{1}{3}}^{\text{diag.}}(\theta \to \pm \infty)$ . However, we can still observe that the unitarity is not satisfied in the small  $\theta$  values, whereas it is satisfied in the large  $\theta$  limit. We can realize how it interpolates between non-unitarity and unitarity continuously from the plot of the matrix elements of  $S(\theta)S(-\theta)$  in Fig.(3.6) and Fig.(3.7). It turns out that this non-unitarity in the small  $\theta$  values is caused by the  $A'_1(\theta)$  and  $A'_2(\theta)$  amplitudes.

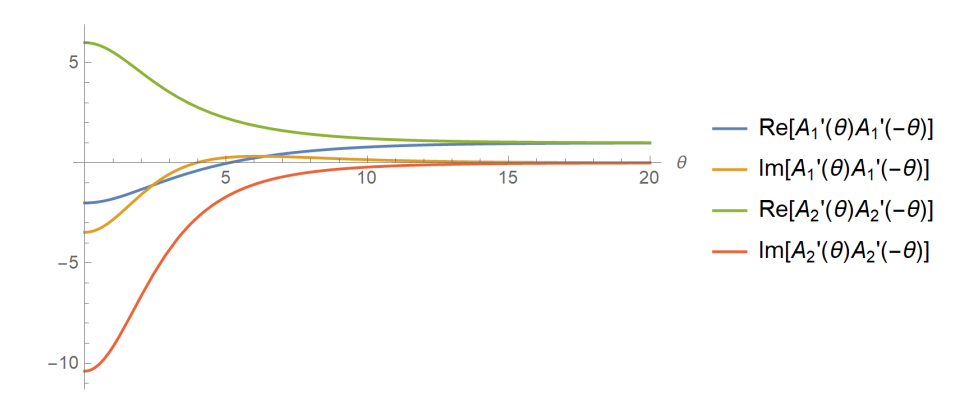


Figure 3.6: The  $\theta$  plot for the rapidity-dependent elements of the unitarity check  $S(\theta)S(-\theta)=\mathbb{I}$  for (3.101).

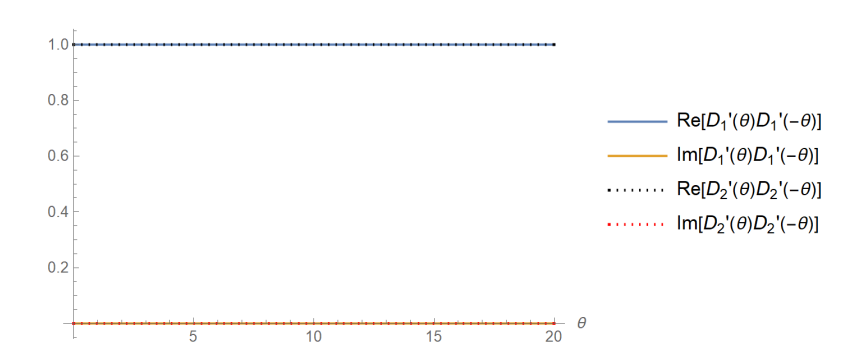


Figure 3.7: The  $\theta$  plot for the rapidity-dependent elements of the unitarity check  $S(\theta)S(-\theta) = \mathbb{I}$  for (3.101).

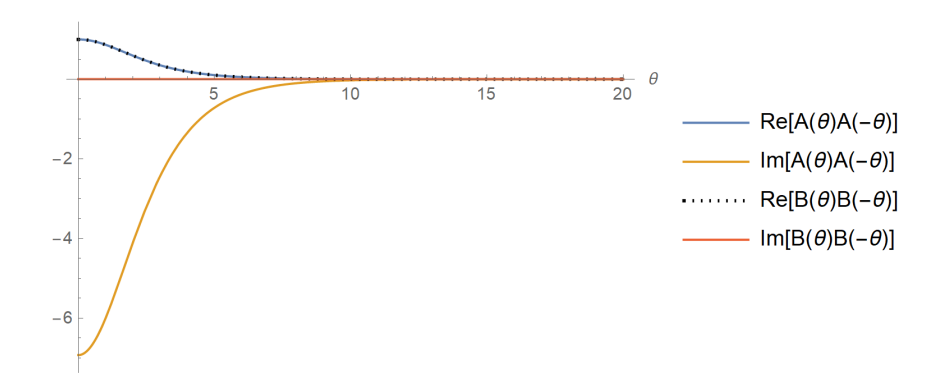


Figure 3.8: The  $\theta$  plot for the rapidity-dependent elements of the unitarity check  $S(\theta)S(-\theta) = \mathbb{I}$  for (3.84).

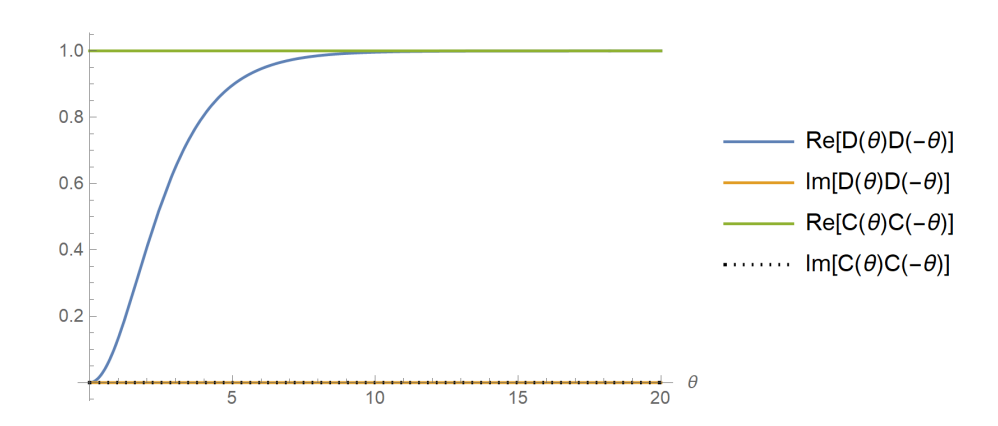
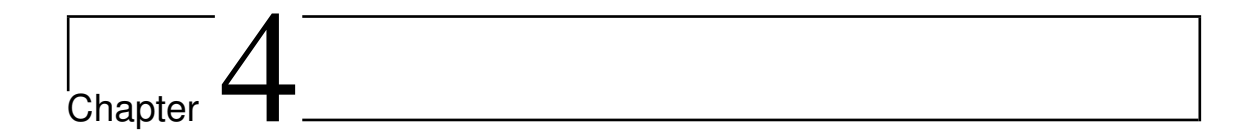


Figure 3.9: The  $\theta$  plot for the rapidity-dependent elements of the unitarity check  $S(\theta)S(-\theta)=\mathbb{I}$  for (3.84).



## Conclusion

The central aim of this thesis has been to investigate the structure and properties of scattering matrices in integrable quantum field theories in 1 + 1 dimensions. Integrability provides an exceptional framework in which scattering processes can be determined exactly, thanks to the presence of infinitely many conserved charges and the resulting constraints on multiparticle interactions. In this setting, factorization of the S-matrix reduces the problem of understanding general scattering to the analysis of two-particle processes, governed by powerful algebraic consistency conditions.

In Chapter 2, we established the theoretical foundation by reviewing scattering theory and the role of S-matrices in integrable models. We analyzed the key structural elements, such as unitarity, analyticity, and crossing symmetry, alongside the Yang–Baxter and bootstrap equations [8, 11, 39]. These principles ensure the consistency of factorized scattering and provide the algebraic machinery through which the S-matrix is constrained. Particular attention was paid to how local conserved charges enforce factorizability and how the Yang–Baxter equation guarantees the associativity of multiparticle scattering, both of which are essential in maintaining integrability.

In Chapter 3, we analyze concrete realizations of factorized scattering. The sine-Gordon model served as a typical example. Its exact S-matrix illustrates how integrability not only yields analytic control but also unifies physical and algebraic perspectives. The sine-Gordon bootstrap program provides a textbook demonstration of how bound states and soliton excitations emerge naturally from consistency conditions [6, 7, 8]. The sausage model, in contrast, showed how the deformations of the integrable theories can produce qualitatively new scattering behavior, but still remain exactly solvable within the integrable framework [34, 37]. This highlighted the strength of the methods and their adaptability to a wide class of models.

The most original part of this thesis focused on higher-spin excitations, in particular, the spin 3/2 case. Here, we constructed and analyzed exact S-matrices for scattering processes involving higher-spin particles, where we extended the integrable machinery to more complex excitations beyond the well-studied spin 1/2 and spin 1 cases. The spin 3/2 construction required careful use of algebraic consistency conditions and provided new insights into how integrability accommodates particles with richer internal structure. In this analysis, a particularly striking result emerged. Even at the "free point", where one would expect scattering to become trivial, the spin 3/2 S-matrix exhibited a nontrivial dependence on rapidity. This behavior is not present in the sine-Gordon or sausage models, where the free point limit corresponds to trivial and rapidity-independent scattering, compatible with bosonic or fermionic exchange [7, 34, 54]. The persistence of rapidity dependence in the free spin 3/2 case suggests a shift from conventional quantum statistics.

Recent advances in the study of non-trivial exchange relations and modified crossing equations provide a natural framework for interpreting this observation. Frolov, Polvara, and Sfondrini [56] have shown that when the free point S-matrix is nontrivial or rapidity-dependent, the underlying excitations typically obey braided statistics rather than standard Bose or Fermi exchange. In such systems, creation and annihilation operators satisfy Zamolodchikov–Faddeev-type exchange relations that encode braiding phases, and the resulting S-matrix inherits these non-standard features. Models such as the SU(N) chiral Gross–Neveu theory and the  $\Phi_{21}$  deformation of tricritical Ising model provide examples for this phenomenon, where

modifications of the crossing equations arise directly from the presence of nontrivial braiding [10, 27, 56]. Our spin 3/2 result thus situates this sector firmly within the emerging class of integrable models with generalized exchange relations.

This discovery brings about several remarkable implications. First, it shows that higher-spin integrable excitations can realize statistics that are qualitatively distinct from those of their lower-spin counterparts, which may suggest a deeper link between spin, integrability, and exchange properties. Second, it opens the possibility that categorical or quantum group symmetries underlie the algebraic structure of these S-matrices, providing a unifying principle for the appearance of braided statistics. Indeed, recent work has linked modified crossing equations to categorical symmetries [56]. This suggests that the braiding observed here may be rooted in such generalized symmetry principles. Third, it proposes the spin 3/2 case as a concrete example where integrability intersects with broader themes in mathematical physics, such as anyonic behavior and the role of generalized statistics in low-dimensional systems.

Beyond its technical significance, the presence of braiding in the spin 3/2 S-matrix enriches the conceptual picture of what integrability can reveal. It underscores that integrable models are not merely solvable toy theories but also testing grounds for discovering new forms of quantum statistics and symmetry principles. This resonates with recent developments in condensed matter physics, where anyonic excitations and braiding are central, as well as in high-energy contexts such as AdS/CFT(for reviews, see [43] and references therein), where integrable structures continue to surface in unexpected ways.

Although the thesis has focused on selected models in dimensions 1+1, the comprehensive picture is that integrability provides both an apparatus for calculations and a medium where new phenomena can be exposed. Future work could pursue several directions. Some of them are the following.

- Systematizing the role of braided statistics in higher-spin theories.
- Exploring possible quantum group or categorical symmetry origins of the braiding.

- Enhancing the bootstrap program to include these nontrivial exchange relations explicitly [55].
- Extending the analysis to models with supersymmetry or to deformations that interpolate between different statistical regimes.
- There is also a possibility of connecting these results with developments in AdS/CFT integrability, particularly via the similarities with modified crossing equations in AdS<sub>3</sub> × S<sub>3</sub> × T<sub>4</sub> models [56].

In a nutshell, this thesis has shown how the combination of integrability and algebraic consistency conditions enables the exact construction of S-matrices in low-dimensional quantum field theories. It has also demonstrated that such constructions do more than solve scattering problems. They also uncover new forms of statistics and deepen our understanding of the relation between symmetry, spin, and integrability. The result that the spin 3/2 case shows braided statistics, even at the "free point", points to a significant step in widening the scope of integrable quantum field theory. By revealing a scenario where higher-spin particles obey exotic exchange rules, this work opens the way for further explorations of braided integrability and its implications across both mathematics and physics.

## Bibliography

- [1] L. Castillejo, R. H. Dalitz, and F. J. Dyson. "Low's Scattering Equation for the Charged and Neutral Scalar Theories". In: *Phys. Rev.* 101 (1 Jan. 1956), pp. 453–458. DOI: 10.1103/PhysRev.101.453.
- [2] G. F. Chew. The Analytic S-Matrix: A Basis for Nuclear Democracy. New York: W. A. Benjamin, 1961.
- [3] C. N. Yang. "Some exact results for the many-body problem in one dimension with repulsive delta-function interaction". In: *Physical Review Letters* 19.23 (1967), pp. 1312–1315. DOI: 10.1103/PhysRevLett.19.1312.
- [4] R. J. Baxter. "Partition function of the eight-vertex lattice model". In: Annals of Physics 70.1 (1972), pp. 193–228. DOI: 10.1016/0003-4916(72)90335-1.
- [5] A. C. Scott, F. Y. F. Chu, and D. W. McLaughlin. "The soliton: A new concept in applied science". In: *Proceedings of the IEEE* 61.10 (1973), pp. 1443–1483. DOI: 10.1109/PROC.1973.9292.
- [6] S. Coleman. "Quantum sine-Gordon equation as the massive Thirring model". In: Physical Review D 11.8 (1975), pp. 2088–2097. DOI: 10.1103/PhysRevD. 11.2088.
- [7] A. B. Zamolodchikov. "Exact Two Particle S-matrix of Quantum Sine-Gordon Solitons". In: Pisma Zh. Eksp. Teor. Fiz. 25 (1977), pp. 499–502. DOI: 10. 1007/BF01626520.

- [8] M. Karowski and P. Weisz. "Exact Form-Factors in (1+1)-Dimensional Field Theoretic Models with Soliton Behavior". In: Nucl. Phys. B 139 (1978), pp. 455– 476. DOI: 10.1016/0550-3213(78)90362-0.
- [9] R. Shankar and Edward Witten. "The S Matrix of the Supersymmetric Non-linear Sigma Model". In: Phys. Rev. D 17 (1978), p. 2134. DOI: 10.1103/PhysRevD.17.2134.
- [10] R. Köberle, V. Kurak, and J. A. Swieca. "Scattering theory and \(\frac{1}{N}\) expansion in the chiral Gross-Neveu model". In: Phys. Rev. D 20 (4 Aug. 1979), pp. 897–902. DOI: 10.1103/PhysRevD.20.897.
- [11] A. B. Zamolodchikov and A. B. Zamolodchikov. "Factorized S-matrices in two dimensions as the exact solutions of certain relativistic quantum field models". In: Annals of Physics 120.2 (1979), pp. 253–291. DOI: 10.1016/0003-4916(79)90391-9.
- [12] Stephen Parke. "Absence of particle production and factorization of the S-matrix in 1 + 1 dimensional models". In: Nuclear Physics B 174.1 (1980), pp. 166–182. ISSN: 0550-3213. DOI: https://doi.org/10.1016/0550-3213(80)90196-0.
- [13] A. B. Zamolodchikov and V. A. Fateev. "Model factorized S-matrix and an integrable spin-1 Heisenberg chain. (in Russian)". In: Sov. J. Nucl. Phys. 32 (1980), pp. 298–303.
- [14] M. J. Ablowitz and H. Segur. Solitons and the Inverse Scattering Transform. SIAM, 1981.
- [15] R. J. Baxter. Exactly Solved Models in Statistical Mechanics. London: Academic Press, 1982.
- [16] R. Rajaraman. Solitons and Instantons: An Introduction to Solitons and Instantons in Quantum Field Theory. North-Holland, 1982.
- [17] L. D. Faddeev. "Integrable models in (1+1)-dimensional quantum field theory". In: Les Houches Summer School 1982. Amsterdam: North-Holland, 1984.

- [18] V. G. Drinfeld. "Hopf algebras and the quantum Yang–Baxter equation". In: Soviet Mathematics Doklady 32 (1985), pp. 254–258.
- [19] V. F. R. Jones. "A polynomial invariant for knots via von Neumann algebras". In: Bulletin of the American Mathematical Society 12.1 (1985), pp. 103–111.
- [20] L. D. Faddeev and L. A. Takhtajan. *Hamiltonian Methods in the Theory of Solitons*. Springer-Verlag, 1987.
- [21] P. G. Drazin and R. S. Johnson. *Solitons: An Introduction*. Cambridge University Press, 1989.
- [22] Michio Jimbo. "Introduction to the Yang–Baxter equation". In: *International Journal of Modern Physics A* 4.15 (1989), pp. 3759–3777. DOI: 10.1142/S0217751X89001503.
- [23] P. Hasenfratz, M. Maggiore, and F. Niedermayer. "The exact mass gap of the O(3) and O(4) non-linear  $\sigma$ -models in d = 2". In: *Physics Letters B* 245.3 (1990), pp. 522–528. ISSN: 0370-2693. DOI: https://doi.org/10.1016/0370-2693(90)90685-Y.
- P. Hasenfratz and F. Niedermayer. "The exact mass gap of the O(N) σ-model for arbitrary N ≥ 3 in d = 2". In: Physics Letters B 245.3 (1990), pp. 529–532.
   ISSN: 0370-2693. DOI: https://doi.org/10.1016/0370-2693(90)90686-Z.
- [25] Timothy R. Klassen and Ezer Melzer. "Purely elastic scattering theories and their ultraviolet limits". In: *Nuclear Physics B* 338.3 (1990), pp. 485–528. ISSN: 0550-3213. DOI: https://doi.org/10.1016/0550-3213(90)90643-R.
- [26] H. Ruegg. "A simple derivation of the quantum Clebsch–Gordan coefficients for  $SU(2)_q$ ". In: Journal of Mathematical Physics 31 (1990), pp. 1085–1092. DOI: 10.1063/1.528819.
- [27] F. A. Smirnov. "Quantum groups and generalized statistics in integrable models". In: Communications in Mathematical Physics 132.2 (1990), pp. 415–439.

- [28] Al.B. Zamolodchikov. "Thermodynamic Bethe ansatz in relativistic models: Scaling 3-state potts and Lee-Yang models". In: *Nuclear Physics B* 342.3 (1990), pp. 695–720. ISSN: 0550-3213. DOI: https://doi.org/10.1016/0550-3213(90)90333-9.
- [29] A. N. Kirillov. "Clebsch–Gordan quantum coefficients". In: *Journal of Soviet Mathematics* 53 (1991), pp. 264–276. DOI: 10.1007/BF01085551.
- [30] T. J. Hollowood. "Solitons in affine Toda field theories". In: *Nuclear Physics B* 384.3 (1992), pp. 523–540. DOI: 10.1016/0550-3213(92)90455-K.
- [31] Bo-Yu Hou, Bo-Yuan Hou, and Zhi-Qiang Ma. "Quantum Clebsch–Gordan coefficients for nongeneric q values". In: Journal of Physics A: Mathematical and General 25 (1992), pp. 1211–1221. DOI: 10.1088/0305-4470/25/5/018.
- [32] F. A. Smirnov. Form Factors in Completely Integrable Models of Quantum Field Theory. World Scientific, 1992.
- [33] A.B. Zamolodchikov and Al.B. Zamolodchikov. "Massless factorized scattering and sigma models with topological terms". In: *Nuclear Physics B* 379.3 (1992), pp. 602–623. ISSN: 0550-3213. DOI: https://doi.org/10.1016/0550-3213(92)90136-Y.
- [34] V. A. Fateev, E. Onofri, and A. B. Zamolodchikov. "Integrable deformations of the O(3) sigma model. The sausage model". In: Nuclear Physics B 406.3 (1993), pp. 521–565. DOI: 10.1016/0550-3213(93)90001-6.
- [35] F. Ravanini, A. Valleriani, and R. Tateo. "Dynkin TBA's". In: *International Journal of Modern Physics A* 08.10 (1993), pp. 1707–1727. DOI: 10.1142/S0217751X93000709.
- [36] S.R. Aladin and M.J. Martins. "Bethe ansatz and thermodynamics of a SU(2)k factorizable S-matrix". In: *Physics Letters B* 329.2 (1994), pp. 271–277. ISSN: 0370-2693. DOI: https://doi.org/10.1016/0370-2693(94)90771-4.

- [37] V.A. Fateev. "The sigma model (dual) representation for a two-parameter family of integrable quantum field theories". In: *Nuclear Physics B* 473.3 (1996), pp. 509–538. ISSN: 0550-3213. DOI: https://doi.org/10.1016/0550-3213(96)00256-8.
- [38] Z. Horváth and G. Takács. "Form-factors of the sausage model obtained with bootstrap fusion from sine-Gordon theory". In: *Physical Review D* 53 (1996), pp. 3272–3284. DOI: 10.1103/PhysRevD.53.3272.
- [39] Patrick Dorey. Exact S-matrices. 1998. arXiv: hep-th/9810026 [hep-th].
- [40] Ph. Blanchard, S. Fortunato, and H. Satz. "The Hagedorn temperature and partition thermodynamics". In: *European Physical Journal C* 34 (2004), pp. 361–366. DOI: 10.1140/epjc/s2004-01673-0.
- [41] R. Rattazzi et al. "Bounding scalar operator dimensions in 4D CFT". In: Journal of High Energy Physics 2008.12 (2008), p. 031. DOI: 10.1088/1126-6708/2008/12/031.
- [42] G. Mussardo. Statistical Field Theory: An Introduction to Exactly Solved Models in Statistical Physics. Oxford: Oxford University Press, 2010.
- [43] Niklas Beisert et al. "Review of AdS/CFT integrability: an overview". In: *Letters in Mathematical Physics* 99.1-3 (2012), pp. 3–32.
- [44] V. Suneeta. "The sausage sigma model revisited". In: Classical and Quantum Gravity 32.11 (2015), p. 115005. DOI: 10.1088/0264-9381/32/11/115005.
- [45] Andrea Cavaglià et al. "TT-deformed 2D quantum field theories". In: *Journal of High Energy Physics* 2016.10 (Oct. 2016). ISSN: 1029-8479. DOI: 10.1007/jhep10(2016)112.
- [46] F.A. Smirnov and A.B. Zamolodchikov. "On space of integrable quantum field theories". In: *Nuclear Physics B* 915 (2017), pp. 363–383. ISSN: 0550-3213. DOI: https://doi.org/10.1016/j.nuclphysb.2016.12.014.

- [47] Vladimir V. Bazhanov, Georgy A. Kotousov, and Sergei L. Lukyanov. "Quantum transfer-matrices for the sausage model". In: *Journal of High Energy Physics* 2018.1 (2018), p. 21. DOI: 10.1007/JHEP01(2018)021.
- [48] Gleb Arutyunov. Elements of Classical and Quantum Integrable Systems. Springer, 2019. DOI: 10.1007/978-3-030-24198-8.
- [49] D. Poland, S. Rychkov, and A. Vichi. "The conformal bootstrap: Theory, numerical techniques, and applications". In: Reviews of Modern Physics 91.1 (2019), p. 015002. DOI: 10.1103/RevModPhys.91.015002.
- [50] G. Mussardo. Statistical Field Theory: Volume 1. Oxford University Press, 2020. ISBN: 978-0198788102.
- [51] Giancarlo Camilo et al. "On factorizable S-matrices, generalized TTbar, and the Hagedorn transition". In: Journal of High Energy Physics 2021.10 (Oct. 2021). ISSN: 1029-8479. DOI: 10.1007/jhep10(2021)062.
- [52] Changrim Ahn and André LeClair. "On the classification of UV completions of integrable  $T\overline{T}$  deformations of CFT". In: Journal of High Energy Physics 2022.8 (Aug. 2022). ISSN: 1029-8479. DOI: 10.1007/jhep08(2022)179.
- [53] Alessandro Torrielli. LonTI Lectures on Sine-Gordon and Thirring. 2022. arXiv: 2211.01186 [hep-th].
- [54] Changrim Ahn, Tommaso Franzini, and Francesco Ravanini. Hagedorn singularity in exact  $U_q(su(2))$  S-matrix theories with arbitrary spins. 2024. arXiv: 2402.15794 [hep-th].
- [55] Christian Copetti, Lucía Córdova, and Shota Komatsu. "S-matrix bootstrap and non-invertible symmetries". In: *Journal of High Energy Physics* 2025.3 (2025), p. 204. DOI: 10.1007/JHEP03(2025)204.
- [56] Sergey Frolov, Davide Polvara, and Alessandro Sfondrini. Exchange relations and crossing. 2025. arXiv: 2506.04096 [hep-th].